Applied Mathematics and Computation 465 (2024) 128410

Contents lists available at ScienceDirect

Applied Mathematics and Computation

journal homepage: www.elsevier.com/locate/amc

Entropy conserving/stable schemes for a vector-kinetic model of hyperbolic systems

Megala Anandan *, S.V. Raghurama Rao

Indian Institute of Science, C.V. Raman Road, 560012, Bangalore, India

ARTICLE INFO

Keywords:
Vector-kinetic model
Entropy conservation
Entropy stability
Hyperbolic system

ABSTRACT

The moment of entropy equation for vector-BGK model results in the entropy equation for macroscopic model. However, this is usually not the case in numerical methods because the current literature consists mostly of entropy conserving/stable schemes for macroscopic model. In this paper, we attempt to fill this gap by developing an entropy conserving scheme for vector-kinetic model, and we show that the moment of this results in an entropy conserving scheme for macroscopic model. With the numerical viscosity of entropy conserving scheme as reference, the entropy stable scheme for vector-kinetic model is developed in the spirit of Tadmor [40]. We show that the moment of this scheme results in an entropy stable scheme for macroscopic model. The schemes are validated on several benchmark test problems for scalar and shallow water equations, and conservation/stability of both kinetic and macroscopic entropies are presented.

1. Introduction

The connection between entropy functions and symmetrisability of hyperbolic systems was explained in [18,19], and this led to entropy-based non-linear stability analysis of numerical schemes. In the seminal work in [40,41], a general condition to conserve/dissipate entropy of a semi-discrete scheme for hyperbolic system was introduced. Following this, many developments on fluxes satisfying entropy conservation/dissipation condition for various hyperbolic systems were made. These include developments specific for shallow water equations [16,43,29], Euler's equations [2,20,32,8,35,36,17,11,10,45], Navier-Stokes equations [44,27,33] and magneto hydro-dynamics equations [9]. Recently, several interesting studies such as, entropy stability for conservation laws with non-convex flux functions [24], and characterisation of stability [15] and robustness (for under-resolved flows) [7] of high order entropy stable schemes were carried out.

On the other hand, kinetic entropy formulations were introduced for hyperbolic equations like multi-dimensional scalar conservation laws, isentropic Euler and full Euler equations [30,25,26,12]. Discrete kinetic models with entropy considerations were also proposed for hyperbolic systems [1,28,4,5,3,6]. Specifically, in [4] it was shown that the entropy inequalities for a hyperbolic system can be derived as minimisation of entropies of vector-kinetic equation with BGK model. This approach of obtaining entropy inequalities from kinetic-BGK models is a promising strategy to characterise weak solutions of hyperbolic systems [31]. Hence, in this paper, we attempt to develop entropy stable schemes (in the sense of [40,41]) for a kinetic model based on [4] and show that they yield entropy stability for the hyperbolic system. This is in contrast to shock capturing schemes [38] based on discrete kinetic models.

A kinetic entropy stable scheme for continuous velocity Boltzmann's equation was recently developed in [21]. Although this scheme

* Corresponding author.
E-mail addresses: megalaa@iisc.ac.in (M. Anandan), raghu@iisc.ac.in (S.V. Raghurama Rao).

https://doi.org/10.1016/j.amc.2023.128410
Received 15 February 2023; Received in revised form 16 August 2023; Accepted 18 October 2023

Available online 28 October 2023

Table 1
Table of symbols.

Symbol	Description
$\mathbf{U}$	Conserved variable vector in macroscopic model
$\mathbf{G}^{(d)}(\mathbf{U})$	Flux vector (along direction d) in macroscopic model
$\eta(\mathbf{U})$	Entropy function for macroscopic model
$\omega^{(d)}(\mathbf{U})$	Entropy flux function for macroscopic model
$\psi^{(d)}$	Entropy flux potential for macroscopic model
$\mathbf{G}^{(d)^\star}_{i_d \pm \frac{1}{2}}$	Entropy conserving interface flux for macroscopic model
$\mathbf{Q}^{(d)^\star}_{i_d \pm \frac{1}{2}}$	Numerical viscosity corresponding to entropy conserving flux for macroscopic model
$\mathbf{G}^{(d)}_{i_d \pm \frac{1}{2}}$	Entropy stable interface flux for macroscopic model
$\mathbf{F}_m$	Dependent variable vector in vector-kinetic model
$v_m^{(d)}$	Discrete velocities in vector-kinetic model
$v_m^{(d)}\mathbf{F}_m$	Flux (along direction d) of the dependent variable vector in vector-kinetic model
H_m^η	Entropy function for vector-kinetic model
$v_m^{(d)} H_m^\eta$	Entropy flux function for vector-kinetic model
$\chi_m^{(d)}$	Entropy flux potential for vector-kinetic model
$\left(v_m^{(d)}\mathbf{F}_m\right)^\star_{i_d \pm \frac{1}{2}}$	Entropy conserving interface flux for vector-kinetic model
$\mathbf{Q}^{(d)^\star}_{m_{i_d \pm \frac{1}{2}}}$	Numerical viscosity corresponding to entropy conserving flux for vector-kinetic model
$\left(v_m^{(d)}\mathbf{F}_m\right)_{i_d \pm \frac{1}{2}}$	Entropy stable interface flux for vector-kinetic model
$\mathbf{V}$	Entropy variable

is entropy stable in the Euler limit, it employs huge number of velocities (24^3 for one dimensional problems) as the velocity space must be sufficiently resolved to satisfy the collision invariance. In our work, due to the usage of discrete kinetic models instead of continuous velocity Boltzmann's equation, we obtain an entropy stable scheme for the vanishing epsilon limit with very few velocities (as low as 2 for one dimensional problems). Moreover, our formalism is general enough to construct entropy stable scheme for a given hyperbolic system, while the work of [21] is specific to the Euler system.
The paper is organised as follows. In section 2, we briefly describe the entropy framework and entropy conservation/stability conditions required to be satisfied by a semi-discrete scheme for hyperbolic system (or macroscopic model). Then, in section 3, we provide a brief description of the vector-BGK model in [4]. In section 4, we describe our modification to vector-BGK model, termed as the vector-kinetic model. This modification allows us to obtain entropy flux potentials required for developing entropy preserving scheme for vector-kinetic model. Then, in sections 5 and 6 we develop entropy conserving and stable schemes for vector-kinetic model, and show that these become entropy conserving and stable schemes for macroscopic model upon taking moments. In section 7, we describe the time discretisation strategies employed to complete our scheme. Then, in section 8, we verify our schemes on various numerical test problems. Section 9 concludes the paper. The list of symbols used in the paper are shown in Table 1.

2. Macroscopic model

Consider the hyperbolic system (or macroscopic model),

$$\partial_t \mathbf{U} + \partial_{x_d} \mathbf{G}^{(d)}(\mathbf{U}) = \mathbf{0} \tag{1}$$

where $\mathbf{U} : \Omega \times [0,T] \to \mathbb{R}^p$ and $\mathbf{G}^{(d)}(\mathbf{U}) : \mathbb{R}^p \to \mathbb{R}^p$, with $d \in \{1,2,..,D\}$. Here Ω is a convex subset of $\mathbb{R}^D$.

2.1. Entropy framework

Here, we briefly recall the underlying theory (presented in [40–42]) behind development of entropy conserving/stable scheme for eq. (1).
If the macroscopic model in eq. (1) admits convex entropy-entropy flux pair $\left(\eta(\mathbf{U}), \omega^{(d)}(\mathbf{U})\right)$ that satisfies,

$$\partial_{\mathbf{U}} \omega^{(d)} = \partial_{\mathbf{U}} \eta \cdot \partial_{\mathbf{U}} \mathbf{G}^{(d)} \Leftrightarrow \partial^2_{\mathbf{U}} \eta \cdot \partial_{\mathbf{U}} \mathbf{G}^{(d)} \text{ is symmetric} \tag{2}$$

then the following entropy inequality holds.

$$\partial_t \eta(\mathbf{U}) + \partial_{x_d} \omega^{(d)}(\mathbf{U}) \leq 0 \tag{3}$$

Equality holds in smooth regions, while strict inequality holds in non-smooth regions.
Due to the convexity of $\eta(\mathbf{U})$, there exists one-one correspondence $\mathbf{U} \to \mathbf{V} := \partial_{\mathbf{U}} \eta$ such that the following equivalent symmetric form of eq. (1) holds true.

$$\partial_{\mathbf{V}}\mathbf{U}\,\partial_t\mathbf{V} + \partial_{\mathbf{U}}\mathbf{G}^{(d)}\,\partial_{\mathbf{V}}\mathbf{U}\,\partial_{x_d}\mathbf{V} = \mathbf{0} \tag{4}$$

Here, $\partial_{\mathbf{V}}\mathbf{U} = \left(\partial^2_{\mathbf{U}}\eta(\mathbf{U})\right)^{-1}$ is symmetric positive-definite (due to the convexity of $\eta(\mathbf{U})$) and $\partial_{\mathbf{V}}\mathbf{G}^{(d)} = \partial_{\mathbf{U}}\mathbf{G}^{(d)}\,\partial_{\mathbf{V}}\mathbf{U}$ is symmetric (refer Harten [18] for theorems due to Godunov and Mock).
Further, the compatibility condition in eq. (2) can be re-written in terms of entropy variable $\mathbf{V}$, thanks to the convexity of $\eta(\mathbf{U})$ that assures existence of $\left(\partial_{\mathbf{U}}\mathbf{V}\right)^{-1}$.

$$\partial_{\mathbf{V}}\omega^{(d)} = \mathbf{V}\cdot\partial_{\mathbf{V}}\mathbf{G}^{(d)} \tag{5}$$

Due to the symmetric nature of $\partial_{\mathbf{V}}\mathbf{G}^{(d)}$, there exist potentials $\psi^{(d)}(\mathbf{V})$ such that $\partial_{\mathbf{V}}\psi^{(d)} = \mathbf{G}^{(d)}(\mathbf{V})$. Therefore, according to eq. (5), there exist entropy flux potentials,

$$\psi^{(d)}(\mathbf{V}) = \mathbf{V}\cdot\mathbf{G}^{(d)}(\mathbf{V}) - \omega^{(d)}(\mathbf{V}) \tag{6}$$

2.2. Entropy conserving scheme

Consider a structured grid with grid size Δx_d along each direction d. Then, a three-point (along each direction d) semi-discrete conservative scheme for eq. (1) is,

$$\frac{d}{dt}\mathbf{U}_i + \frac{1}{\Delta x_d}\left(\mathbf{G}^{(d)\star}_{i_d+\frac{1}{2}} - \mathbf{G}^{(d)\star}_{i_d-\frac{1}{2}}\right) = \mathbf{0} \tag{7}$$

Here i denotes the index for cell centre of each cell/finite volume, and $i_d \pm \frac{1}{2}$ denote indices for right/left interfaces of cell i along direction d. For consistency, the numerical flux $\mathbf{G}^{(d)\star}_{i_d\pm\frac{1}{2}} := \mathbf{G}^{(d)\star}_{i_d\pm\frac{1}{2}}\left(\mathbf{U}_i, \mathbf{U}_{i_d\pm1}\right)$ is such that $\mathbf{G}^{(d)\star}_{i_d\pm\frac{1}{2}}(\mathbf{U},\mathbf{U}) = \mathbf{G}^{(d)}(\mathbf{U})$, where $i_d \pm 1$ denote indices for the cell centres of cells to the right/left of cell i along direction d.
The scheme in eq. (7) is entropy conserving iff the interface numerical fluxes satisfy the entropy conserving condition (derived in [40,41]),

$$\left\langle [[\mathbf{V}]]_{i_d+\frac{1}{2}}, \mathbf{G}^{(d)\star}_{i_d+\frac{1}{2}} \right\rangle = \left[\left[\psi^{(d)}\right]\right]_{i_d+\frac{1}{2}} \tag{8}$$

Here, $[[(.)]]_{i_d+\frac{1}{2}}$ denotes the jump $(.)_{i_d+1} - (.)_i$. Then, the following three-point (along each direction d) entropy equality holds true.

$$\frac{d}{dt}\eta\left(\mathbf{V}_i\right) + \frac{1}{\Delta x_d}\left(\omega^{(d)\star}_{i_d+\frac{1}{2}} - \omega^{(d)\star}_{i_d-\frac{1}{2}}\right) = 0 \tag{9}$$

The interface numerical entropy flux consistent with eq. (6) is given by

$$\omega^{(d)\star}_{i_d\pm\frac{1}{2}} = \frac{1}{2}\left(\mathbf{V}_i + \mathbf{V}_{i_d\pm1}\right)\cdot\mathbf{G}^{(d)\star}_{i_d\pm\frac{1}{2}} - \frac{1}{2}\left(\psi^{(d)}_i + \psi^{(d)}_{i_d\pm1}\right) \tag{10}$$

Further, the entropy conserving numerical flux $\mathbf{G}^{(d)\star}_{i_d+\frac{1}{2}}$ satisfying eq. (8) can be evaluated along the path $\mathbf{V}_{i_d+\frac{1}{2}}(\xi) = \mathbf{V}_i + \xi\Delta\mathbf{V}_{i_d+\frac{1}{2}}$ as,

$$\mathbf{G}^{(d)\star}_{i_d\pm\frac{1}{2}} = \frac{1}{2}\left(\mathbf{G}^{(d)}_i + \mathbf{G}^{(d)}_{i_d\pm1}\right) - \frac{1}{2}\mathbf{Q}^{(d)\star}_{i_d\pm\frac{1}{2}}\,[[\mathbf{V}]]_{i_d\pm\frac{1}{2}} \tag{11}$$

with

$$\mathbf{Q}^{(d)\star}_{i_d+\frac{1}{2}} = \int_0^1 (2\xi-1)\,\partial_{\mathbf{V}}\mathbf{G}^{(d)}\left(\mathbf{V}_{i_d+\frac{1}{2}}(\xi)\right)d\xi \tag{12}$$

The term $\mathbf{Q}^{(d)\star}_{i_d\pm\frac{1}{2}}$ which is symmetric (need not be positive-definite) is considered as numerical viscosity coefficient matrix. This counterbalances dispersion from the average flux. Further, the entropy conserving scheme is second order accurate in space (refer [40,41]). Construction of higher order entropy conserving fluxes as linear combinations of second order accurate entropy conserving fluxes $\mathbf{G}^{(d)\star}_{i_d\pm\frac{1}{2}}$ is discussed in [23].

2.3. Entropy stable scheme

The three-point (along each direction d) consistent flux,

$$\mathbf{G}^{(d)}_{i_d\pm\frac{1}{2}} = \mathbf{G}^{(d)\star}_{i_d\pm\frac{1}{2}} - \frac{1}{2}\mathbf{D}^{(d)}_{i_d\pm\frac{1}{2}}\,[[\mathbf{V}]]_{i_d\pm\frac{1}{2}} \tag{13}$$

with $\mathbf{D}^{(d)}_{i_d\pm\frac{1}{2}} = \mathbf{Q}^{(d)}_{i_d\pm\frac{1}{2}} - \mathbf{Q}^{(d)\star}_{i_d\pm\frac{1}{2}}$ is entropy stable if and only if $\mathbf{D}^{(d)}_{i_d\pm\frac{1}{2}}$ is positive-definite. Here $\mathbf{Q}^{(d)}_{i_d\pm\frac{1}{2}}$ is the numerical viscosity coefficient matrix corresponding to entropy stable scheme. The scheme then satisfies the three-point entropy inequality,

$$\frac{d}{dt}\eta\left(\mathbf{V}_i\right)+\frac{1}{\Delta x_d}\left(\omega^{(d)}_{i_d+\frac{1}{2}}-\omega^{(d)}_{i_d-\frac{1}{2}}\right)=-\frac{1}{4\Delta x_d}\left(\left[[\mathbf{V}]\right]_{i_d+\frac{1}{2}}\cdot\mathbf{D}^{(d)}_{i_d+\frac{1}{2}}\left[[\mathbf{V}]\right]_{i_d+\frac{1}{2}}+\left[[\mathbf{V}]\right]_{i_d-\frac{1}{2}}\cdot\mathbf{D}^{(d)}_{i_d-\frac{1}{2}}\left[[\mathbf{V}]\right]_{i_d-\frac{1}{2}}\right)\leq 0 \tag{14}$$

Here, the consistent numerical entropy flux at interface is given by,

$$\omega^{(d)}_{i_d+\frac{1}{2}}=\omega^{(d)\star}_{i_d+\frac{1}{2}}-\frac{1}{4}\left(\mathbf{V}_i+\mathbf{V}_{i_d+1}\right)\cdot\mathbf{D}^{(d)}_{i_d+\frac{1}{2}}\left[[\mathbf{V}]\right]_{i_d+\frac{1}{2}} \tag{15}$$

The entropy stable flux $\mathbf{G}^{(d)}_{i_d\pm\frac{1}{2}}$ given by eq. (13) is first order accurate in space (refer Tadmor [40,41]). To achieve higher order accuracy in space, the term $\left[[\mathbf{V}]\right]_{i_d+\frac{1}{2}}$ in eq. (13) must be replaced by $\langle\langle\mathbf{V}\rangle\rangle_{i_d+\frac{1}{2}}=\mathbf{V}^-_{i_d+1}-\mathbf{V}^+_i$ where $\mathbf{V}^-_{i_d+1}$ and $\mathbf{V}^+_i$ are higher order reconstructions of $\mathbf{V}$ at interface $i_d+\frac{1}{2}$ (refer [14]).

3. Vector-BGK model

In this section, we briefly describe the vector-BGK model presented in [4]. Consider,

$$\partial_t\mathbf{f}_m+\partial_{x_d}\left(v^{(d)}_m\mathbf{f}_m\right)=-\frac{1}{\epsilon}\left(\mathbf{f}_m-\mathbf{F}_m(\mathbf{U})\right) \tag{16}$$

where ϵ is the relaxation parameter. Here, $\mathbf{f}_m:=\mathbf{f}_m(x_1,..,x_d,..,x_D,v^{(1)}_m,..,v^{(d)}_m,..,v^{(D)}_m,t)\in\mathbb{R}^p$, $\mathbf{F}_m:\mathbb{R}^p\to\mathbb{R}^p$, $m\in\{1,2,..,M\}$ and M is the number of discrete velocities. Splitting of streaming and relaxation operators in eq. (16) gives,

$$\text{Streaming: } \partial_t\mathbf{f}_m+\partial_{x_d}\left(v^{(d)}_m\mathbf{f}_m\right)=\mathbf{0} \tag{17}$$

$$\text{Relaxation: } \frac{d}{dt}\mathbf{f}_m=-\frac{1}{\epsilon}\left(\mathbf{f}_m-\mathbf{F}_m(\mathbf{U})\right) \tag{18}$$

Instantaneous relaxation (i.e., $\epsilon=0$) in the relaxation equation above yields $\mathbf{f}_m=\mathbf{F}_m(\mathbf{U})$. This is inserted into the streaming equation for its evolution. Now, it can be seen that if the following relations are satisfied,

$$\sum_{m=1}^{M}\mathbf{F}_m(\mathbf{U})=\mathbf{U}\text{ and }\sum_{m=1}^{M}v^{(d)}_m\mathbf{F}_m(\mathbf{U})=\mathbf{G}^{(d)}(\mathbf{U}) \tag{19}$$

then $\sum_{m=1}^{M}$ eq. (16) $\to$ eq. (1) as $\epsilon\to 0$.

3.1. Entropy framework

Following the definition of entropy function for vector-BGK model given by equations (E0)-(E2) in [4], let us define the entropy function $H^\eta_m\left(\mathbf{f}_m\right)$ as:

$$H^\eta_m\left(\mathbf{f}_m\right)\text{ is a convex function with respect to }\mathbf{f}_m \tag{20}$$

$$\sum_{m=1}^{M}H^\eta_m\left(\mathbf{F}_m(\mathbf{U})\right)=\eta(\mathbf{U}) \tag{21}$$

$$\sum_{m=1}^{M}H^\eta_m\left(\mathbf{F}_m(\mathbf{U})\right)\leq\sum_{m=1}^{M}H^\eta_m\left(\mathbf{f}_m\right) \tag{22}$$

Then, taking inner product of eq. (16) with the sub-differential of H^η_m at $\mathbf{F}_m(\mathbf{U})$ and using (20), (21) and (22), the following is obtained.

$$\begin{aligned}\partial_t H^\eta_m(\mathbf{f}_m)+\partial_{x_d}\left(v^{(d)}_m H^\eta_m(\mathbf{f}_m)\right)\leq\frac{1}{\epsilon}\left(H^\eta_m\left(\mathbf{F}_m(\mathbf{U})\right)-H^\eta_m\left(\mathbf{f}_m\right)\right)\\ \Rightarrow\sum_{m=1}^{M}\left(\partial_t H^\eta_m(\mathbf{f}_m)+\partial_{x_d}\left(v^{(d)}_m H^\eta_m(\mathbf{f}_m)\right)\right)\leq 0\\ \Rightarrow\partial_t\eta(\mathbf{U})+\partial_{x_d}\left(\sum_{m=1}^{M}v^{(d)}_m H^\eta_m(\mathbf{F}_m(\mathbf{U}))\right)\leq 0\text{ in the limit }\epsilon\to 0\end{aligned} \tag{23}$$

If $\omega^{(d)}(\mathbf{U})=\sum_{m=1}^{M}v^{(d)}_m H^\eta_m(\mathbf{F}_m(\mathbf{U}))$, then eq. (23) is same as eq. (3). The reader is referred to [4] for details.
Thus, entropy inequality of the macroscopic model (eq. (1)) can be obtained as minimisation of entropies of the vector-BGK model (eq. (16)). This inspires one to develop entropy structure preserving numerical schemes for vector-BGK model that recover the entropy inequality of equivalent macroscopic scheme. However, the framework of vector-BGK model does not ensure the existence of $\partial^2_{\mathbf{f}_m}H^\eta_m\left(\mathbf{F}_m(\mathbf{U})\right)$ which is crucial in obtaining entropy flux potentials that allow for the consistent definition of interface numerical entropy fluxes. Hence, we resort to a much simpler model in the relaxed limit without the stiff relaxation parameter (hereafter referred as *vector-kinetic model*), and make the necessary modification to allow for the definition of entropy flux potentials.

4. Vector-kinetic model

In this model, we consider the evolution of relaxed limit ($\epsilon = 0$):

$$\partial_t \mathbf{F}_m + \partial_{x_d}\left(v_m^{(d)}\mathbf{F}_m\right) = \mathbf{0} \tag{24}$$

Let us define $\mathbf{F}_m(\mathbf{U})$ as in [4],

$$\mathbf{F}_m(\mathbf{U}) = a_m\mathbf{U} + b_m^{(d)}\mathbf{G}^{(d)}(\mathbf{U}) \tag{25}$$

with

$$\sum_{m=1}^{M} a_m = 1,\ \sum_{m=1}^{M} b_m^{(d)} = 0 \tag{26}$$

$$\sum_{m=1}^{M} v_m^{(j)} a_m = 0,\ \sum_{m=1}^{M} v_m^{(j)} b_m^{(d)} = \delta_{jd} \tag{27}$$

In the light of moment constraints in eqs. (26) and (27), the definition of $\mathbf{F}_m(\mathbf{U})$ in eq. (25) satisfies eq. (19).

4.1. Entropy framework

Define H_m^η as in [4],

$$H_m^\eta(\mathbf{U}) = a_m\eta(\mathbf{U}) + b_m^{(d)}\omega^{(d)}(\mathbf{U}) \tag{28}$$

Due to the constraints in eqs. (26) and (27), H_m^η satisfies,

$$\sum_{m=1}^{M} H_m^\eta(\mathbf{U}) = \eta(\mathbf{U}) \text{ and } \sum_{m=1}^{M} v_m^{(d)} H_m^\eta(\mathbf{U}) = \omega^{(d)}(\mathbf{U}) \tag{29}$$

We assume that the eigenvalues of $\partial_{\mathbf{U}}\mathbf{F}_m$ are positive, unlike in [4] where the eigenvalues are considered to be non-negative. It will be seen that this modification allows the definition of entropy flux potentials required in the construction of entropy preserving numerical scheme. As $\partial_{\mathbf{U}}\mathbf{F}_m$ is now invertible, $\partial_{\mathbf{F}_m} H_m^\eta$ satisfying $\partial_{\mathbf{U}} H_m^\eta = \partial_{\mathbf{F}_m} H_m^\eta \cdot \partial_{\mathbf{U}}\mathbf{F}_m$ exists. Therefore, the inner product of eq. (24) with $\partial_{\mathbf{F}_m} H_m^\eta$ gives,

$$\partial_t H_m^\eta + \partial_{x_d}\left(v_m^{(d)} H_m^\eta\right) = 0 \tag{30}$$

It can be seen that $\sum_{m=1}^{M}$ (eq. (30)) becomes eq. (3) with equality. Motivated by this, in this paper, we develop entropy preserving scheme for vector-kinetic model that recovers entropy preservation of equivalent macroscopic scheme.

Lemma 1. *If $\mathbf{F}_m(\mathbf{U})$ and $H_m^\eta(\mathbf{U})$ respectively follow eqs. (25) and (28) with constants a_m, $b_m^{(d)}$ satisfying the moment constraints in eqs. (26) and (27) and rendering the eigenvalues of $\partial_{\mathbf{U}}\mathbf{F}_m$ to be positive, then $\partial_{\mathbf{F}_m} H_m^\eta = \partial_{\mathbf{U}}\eta$.*

Proof. Due to the compatibility condition in eq. (2), it can be seen from differentiation (with respect to $\mathbf{U}$) of eqs. (25) and (28) that $\partial_{\mathbf{U}} H_m^\eta = \partial_{\mathbf{U}}\eta \cdot \partial_{\mathbf{U}}\mathbf{F}_m$. Since $\partial_{\mathbf{U}}\mathbf{F}_m$ is invertible, $\partial_{\mathbf{U}}\eta = \partial_{\mathbf{U}} H_m^\eta \cdot \left(\partial_{\mathbf{U}}\mathbf{F}_m\right)^{-1}$. We already saw that $\partial_{\mathbf{F}_m} H_m^\eta = \partial_{\mathbf{U}} H_m^\eta \cdot \left(\partial_{\mathbf{U}}\mathbf{F}_m\right)^{-1}$. □

This lemma shows that the entropy variables for macroscopic and vector-kinetic models are equal, *i.e.,*

$$\mathbf{V} = \partial_{\mathbf{U}}\eta = \partial_{\mathbf{F}_m} H_m^\eta. \tag{31}$$

The choice of constants a_m, $b_m^{(d)}$ satisfying assumptions in the above lemma are discussed in Appendix A.
As a consequence of Lemma 1, we have $\partial^2_{\mathbf{F}_m} H_m^\eta = \partial^2_{\mathbf{U}}\eta \cdot \left(\partial_{\mathbf{U}}\mathbf{F}_m\right)^{-1}$. Further, $\left(\partial^2_{\mathbf{U}}\eta\right)^{-1} \partial^2_{\mathbf{F}_m} H_m^\eta = \left(\partial_{\mathbf{U}}\mathbf{F}_m\right)^{-1}$ can be expressed as

$$\left(\partial^2_{\mathbf{U}}\eta\right)^{-\frac{1}{2}} \left(\partial^2_{\mathbf{U}}\eta\right)^{-\frac{1}{2}} \left(\partial^2_{\mathbf{F}_m} H_m^\eta\right) \left(\partial^2_{\mathbf{U}}\eta\right)^{-\frac{1}{2}} \left(\partial^2_{\mathbf{U}}\eta\right)^{\frac{1}{2}} = \left(\partial_{\mathbf{U}}\mathbf{F}_m\right)^{-1} \tag{32}$$

thanks to the positive-definiteness of $\partial^2_{\mathbf{U}}\eta$. Thus, $\left(\partial^2_{\mathbf{U}}\eta\right)^{-\frac{1}{2}} \left(\partial^2_{\mathbf{F}_m} H_m^\eta\right) \left(\partial^2_{\mathbf{U}}\eta\right)^{-\frac{1}{2}}$ and $\left(\partial_{\mathbf{U}}\mathbf{F}_m\right)^{-1}$ are similar and therefore their eigenvalues are same.

Lemma 2. *If $\partial^2_{\mathbf{U}}\eta$ is positive-definite and eq. (32) holds true, then $\partial^2_{\mathbf{F}_m} H_m^\eta$ is positive-definite iff the eigenvalues of $\left(\partial_{\mathbf{U}}\mathbf{F}_m\right)^{-1}$ are positive.*

Proof. $\left(\partial^2_{\mathbf{U}}\eta\right)^{-\frac{1}{2}} \left(\partial^2_{\mathbf{F}_m} H_m^\eta\right) \left(\partial^2_{\mathbf{U}}\eta\right)^{-\frac{1}{2}}$ is symmetric as $\partial^2_{\mathbf{U}}\eta$ and $\partial^2_{\mathbf{F}_m} H_m^\eta$ are symmetric. Further, we have $\forall \mathbf{y} \neq \mathbf{0} \in \mathbb{R}^p$,

$$\mathbf{y} \cdot \left(\partial^2_{\mathbf{U}}\eta\right)^{-\frac{1}{2}} \left(\partial^2_{\mathbf{F}_m} H_m^\eta\right) \left(\partial^2_{\mathbf{U}}\eta\right)^{-\frac{1}{2}} \mathbf{y} = \mathbf{z} \cdot \left(\partial^2_{\mathbf{F}_m} H_m^\eta\right) \mathbf{z} \tag{33}$$

where $\mathbf{z} = \left(\partial^2_{\mathbf{U}}\eta\right)^{-\frac{1}{2}}\mathbf{y} \neq \mathbf{0}$ (as $\partial^2_{\mathbf{U}}\eta$ is positive-definite).

$\Leftarrow$ If the eigenvalues of $\left(\partial_{\mathbf{U}}\mathbf{F}_m\right)^{-1}$ are positive, then $\left(\partial^2_{\mathbf{U}}\eta\right)^{-\frac{1}{2}}\left(\partial^2_{\mathbf{F}_m}H^\eta_m\right)\left(\partial^2_{\mathbf{U}}\eta\right)^{-\frac{1}{2}}$ is positive-definite due to eq. (32). Then $\partial^2_{\mathbf{F}_m}H^\eta_m$ is rendered positive-definite by eq. (33).

$\Rightarrow$ If $\partial^2_{\mathbf{F}_m}H^\eta_m$ is positive-definite, then by eq. (33) $\left(\partial^2_{\mathbf{U}}\eta\right)^{-\frac{1}{2}}\left(\partial^2_{\mathbf{F}_m}H^\eta_m\right)\left(\partial^2_{\mathbf{U}}\eta\right)^{-\frac{1}{2}}$ is positive-definite. Then, the eigenvalues of $\left(\partial_{\mathbf{U}}\mathbf{F}_m\right)^{-1}$ are positive due to eq. (32). □

Thus, as consequence of Lemma 1 and Lemma 2, eq. (31) and positive-definiteness of $\partial^2_{\mathbf{F}_m}H^\eta_m$ are guaranteed iff the eigenvalues of $\partial_{\mathbf{U}}\mathbf{F}_m$ are positive. Using the one-to-one correspondence between $\mathbf{U}$ and $\mathbf{V}$, we consider $\mathbf{F}_m(\mathbf{U}) = \mathbf{F}_m(\mathbf{U}(\mathbf{V}))$. Hence the vector-kinetic model in eq. (24) can be expressed in the equivalent symmetric form

$$\partial_{\mathbf{V}}\mathbf{F}_m\partial_t\mathbf{V} + \partial_{\mathbf{V}}\left(\upsilon^{(d)}_m\mathbf{F}_m\right)\partial_{x_d}\mathbf{V} = \mathbf{0} \tag{34}$$

Here $\partial_{\mathbf{V}}\mathbf{F}_m = \left(\partial^2_{\mathbf{F}_m}H^\eta_m\right)^{-1}$ is symmetric positive-definite. Due to the linearity of vector-kinetic model, $\partial_{\mathbf{V}}\left(\upsilon^{(d)}_m\mathbf{F}_m\right) = \upsilon^{(d)}_m\partial_{\mathbf{V}}\mathbf{F}_m$ is symmetric. As a result, there exist potentials $\chi^{(d)}_m(\mathbf{V})$ such that

$$\partial_{\mathbf{V}}\chi^{(d)}_m = \upsilon^{(d)}_m\mathbf{F}_m \tag{35}$$

Further, the compatibility condition

$$\partial_{\mathbf{F}_m}\left(\upsilon^{(d)}_m H^\eta_m\right) = \partial_{\mathbf{F}_m}H^\eta_m\cdot\partial_{\mathbf{F}_m}\left(\upsilon^{(d)}_m\mathbf{F}_m\right) \tag{36}$$

is also satisfied rendering H^η_m as the convex entropy function for vector-kinetic model. Note that this compatibility condition is always true for any convex H^η_m satisfying eq. (28) due to the linear nature of vector-kinetic model, unlike the compatibility condition (eq. (2)) for macroscopic model. In terms of $\mathbf{V}$, the above compatibility condition for vector-kinetic model becomes,

$$\partial_{\mathbf{V}}\left(\upsilon^{(d)}_m H^\eta_m\right) = \mathbf{V}\cdot\partial_{\mathbf{V}}\left(\upsilon^{(d)}_m\mathbf{F}_m\right) \tag{37}$$

thanks to the inverse of $\partial_{\mathbf{F}_m}\mathbf{V}$. Therefore, due to eqs. (35) and (37), there exist entropy flux potentials

$$\chi^{(d)}_m(\mathbf{V}) = \mathbf{V}\cdot\upsilon^{(d)}_m\mathbf{F}_m - \upsilon^{(d)}_m H^\eta_m = \partial_{\mathbf{F}_m}H^\eta_m\cdot\upsilon^{(d)}_m\mathbf{F}_m - \upsilon^{(d)}_m H^\eta_m \tag{38}$$

Thus, we have obtained the entropy flux potentials that are crucial in the construction of entropy preserving numerical scheme for vector-kinetic model.

5. Entropy conserving scheme for vector-kinetic model

The three-point (along each direction d) semi-discrete conservative scheme for vector-kinetic model in eq. (24) on a structured grid is given by,

$$\frac{d}{dt}\mathbf{F}_{m_i} + \frac{1}{\Delta x_d}\left(\left(\upsilon^{(d)}_m\mathbf{F}_m\right)^\star_{i_d+\frac{1}{2}} - \left(\upsilon^{(d)}_m\mathbf{F}_m\right)^\star_{i_d-\frac{1}{2}}\right) = \mathbf{0} \tag{39}$$

Here, $\mathbf{F}_{m_i}(t) = \mathbf{F}_m\left(\mathbf{V}_i(t)\right)$ and consistent $\left(\upsilon^{(d)}_m\mathbf{F}_m\right)^\star_{i_d+\frac{1}{2}} = \upsilon^{(d)}_m\mathbf{F}_m(\mathbf{V}_i,\mathbf{V}_{i_d+1})$ is such that $\upsilon^{(d)}_m\mathbf{F}_m(\mathbf{V},\mathbf{V}) = \upsilon^{(d)}_m\mathbf{F}_m(\mathbf{V})$. Consider the inner product $\left(\partial_{\mathbf{F}_m}H^\eta_m\right)_i\cdot\left(\upsilon^{(d)}_m\mathbf{F}_m\right)^\star_{i_d\pm\frac{1}{2}}$:

$$\begin{aligned}\left(\partial_{\mathbf{F}_m}H^\eta_m\right)_i\cdot\left(\upsilon^{(d)}_m\mathbf{F}_m\right)^\star_{i_d\pm\frac{1}{2}} &= \frac{1}{2}\left(\left(\partial_{\mathbf{F}_m}H^\eta_m\right)_{i_d\pm1} + \left(\partial_{\mathbf{F}_m}H^\eta_m\right)_i\right)\cdot\left(\upsilon^{(d)}_m\mathbf{F}_m\right)^\star_{i_d\pm\frac{1}{2}}\\ &\quad -\frac{1}{2}\left(\left(\partial_{\mathbf{F}_m}H^\eta_m\right)_{i_d\pm1} - \left(\partial_{\mathbf{F}_m}H^\eta_m\right)_i\right)\cdot\left(\upsilon^{(d)}_m\mathbf{F}_m\right)^\star_{i_d\pm\frac{1}{2}}\end{aligned}$$

If the interface numerical flux $\left(\upsilon^{(d)}_m\mathbf{F}_m\right)^\star_{i_d+\frac{1}{2}}$ satisfies the entropy conserving condition,

$$\left\langle\left[\left[\partial_{\mathbf{F}_m}H^\eta_m\right]\right]_{i_d+\frac{1}{2}}, \left(\upsilon^{(d)}_m\mathbf{F}_m\right)^\star_{i_d+\frac{1}{2}}\right\rangle = \left[\left[\chi^{(d)}_m\right]\right]_{i_d+\frac{1}{2}} \tag{40}$$

then,

$$\left(\partial_{\mathbf{F}_m}H^\eta_m\right)_i\cdot\left(\upsilon^{(d)}_m\mathbf{F}_m\right)^\star_{i_d\pm\frac{1}{2}} = \frac{1}{2}\left(\left(\partial_{\mathbf{F}_m}H^\eta_m\right)_{i_d\pm1} + \left(\partial_{\mathbf{F}_m}H^\eta_m\right)_i\right)\cdot\left(\upsilon^{(d)}_m\mathbf{F}_m\right)^\star_{i_d\pm\frac{1}{2}} - \frac{1}{2}\left(\chi^{(d)}_{m_{i_d\pm1}} - \chi^{(d)}_{m_i}\right)$$

Thus, the inner product of eq. (39) with $\left(\partial_{\mathbf{F}_m}H^\eta_m\right)_i$ gives the three-point entropy equality,

$$\frac{d}{dt}H^{\eta}_{m_i} + \frac{1}{\Delta x_d}\left(\left(v^{(d)}_m H^{\eta}_m\right)^{\star}_{i_d+\frac{1}{2}} - \left(v^{(d)}_m H^{\eta}_m\right)^{\star}_{i_d-\frac{1}{2}}\right) = 0 \tag{41}$$

iff it satisfies eq. (40), and the interface numerical entropy fluxes $\left(v^{(d)}_m H^{\eta}_m\right)^{\star}_{i_d\pm\frac{1}{2}}$ consistent with eq. (38) are given by,

$$\left(v^{(d)}_m H^{\eta}_m\right)^{\star}_{i_d\pm\frac{1}{2}} = \frac{1}{2}\left(\left(\partial_{\mathbf{F}_m} H^{\eta}_m\right)_i + \left(\partial_{\mathbf{F}_m} H^{\eta}_m\right)_{i_d\pm 1}\right)\cdot\left(v^{(d)}_m \mathbf{F}_m\right)^{\star}_{i_d\pm\frac{1}{2}} - \frac{1}{2}\left(\chi^{(d)}_{m_i} + \chi^{(d)}_{m_{i_d\pm 1}}\right) \tag{42}$$

It is seen that the entropy flux potentials $\chi^{(d)}_{m_i}$ enable us to consistently relate the two interfacial unknowns, numerical fluxes $\left(v^{(d)}_m \mathbf{F}_m\right)^{\star}_{i_d\pm\frac{1}{2}}$ and numerical entropy fluxes $\left(v^{(d)}_m H^{\eta}_m\right)^{\star}_{i_d\pm\frac{1}{2}}$. Further, let us define the interface numerical fluxes for macroscopic model as the moment of interface numerical fluxes for vector-kinetic model as,

$$\mathbf{G}^{(d)^{\star}}_{i_d\pm\frac{1}{2}} = \sum_{m=1}^{M}\left(v^{(d)}_m \mathbf{F}_m\right)^{\star}_{i_d\pm\frac{1}{2}} \tag{43}$$

Theorem 1. *If the three-point semi-discrete conservative scheme (eq. (39)) for vector-kinetic model with*

- $\mathbf{F}_{m_i} = a_m \mathbf{U}_i + b^{(d)}_m \mathbf{G}^{(d)}_i,\ \forall i$
- *interface numerical fluxes* $\left(v^{(d)}_m \mathbf{F}_m\right)^{\star}_{i_d\pm\frac{1}{2}}$ *satisfying the entropy conserving condition in eq. (40) and*
- *constants* a_m, $b^{(d)}_m$ *satisfying the moment constraints in eqs. (26) and (27) while rendering positivity of eigenvalues of* $\partial_{\mathbf{U}}\mathbf{F}_m$

is used, and if the convex entropy function corresponding to it is $H^{\eta}_{m_i} = a_m \eta_i + b^{(d)}_m \omega^{(d)}_i,\ \forall i$, *then*

1. $\sum_{m=1}^{M}$ *(eq. (39)) becomes*

$$\frac{d}{dt}\mathbf{U}_i + \frac{1}{\Delta x_d}\left(\mathbf{G}^{(d)^{\star}}_{i_d+\frac{1}{2}} - \mathbf{G}^{(d)^{\star}}_{i_d-\frac{1}{2}}\right) = \mathbf{0} \tag{44}$$

   with $\mathbf{G}^{(d)^{\star}}_{i_d\pm\frac{1}{2}}$ *given by eq. (43),*
2. *the interface numerical flux* $\mathbf{G}^{(d)^{\star}}_{i_d\pm\frac{1}{2}}$ *given by eq. (43) satisfies the entropy conserving condition for macroscopic model (eq. (8)), and*
3. *the three-point entropy equality for macroscopic model (eq. (9)) holds true with interface numerical entropy flux* $\omega^{(d)^{\star}}_{i_d\pm\frac{1}{2}}$ *given by eq. (10).*

Proof. Due to moment constraint in eq. (26), $\sum_{m=1}^{M}\mathbf{F}_{m_i} = \mathbf{U}_i$. Therefore, $\sum_{m=1}^{M}$ (eq. (39)) becomes eq. (44) with $\mathbf{G}^{(d)^{\star}}_{i_d\pm\frac{1}{2}}$ given by eq. (43), thus proving 1.
By eq. (31), $\left[\left[\partial_{\mathbf{F}_m} H^{\eta}_m\right]\right]_{i_d\pm\frac{1}{2}} = [[\mathbf{V}]]_{i_d\pm\frac{1}{2}} = \left[\left[\partial_{\mathbf{U}}\eta\right]\right]_{i_d\pm\frac{1}{2}}$ is not a function of m. Hence, the moment of eq. (40) gives,

$$\left\langle [[\mathbf{V}]]_{i_d\pm\frac{1}{2}}, \sum_{m=1}^{M}\left(v^{(d)}_m \mathbf{F}_m\right)^{\star}_{i_d\pm\frac{1}{2}}\right\rangle = \left[\left[\sum_{m=1}^{M}\chi^{(d)}_m\right]\right]_{i_d\pm\frac{1}{2}} \tag{45}$$

From eq. (38), it can be seen that $\chi^{(d)}_{m_i} = \mathbf{V}_i . v^{(d)}_m \mathbf{F}_{m_i} - v^{(d)}_m H^{\eta}_{m_i},\ \forall i$. Hence, $\sum_{m=1}^{M}\chi^{(d)}_{m_i} = \mathbf{V}_i . \sum_{m=1}^{M}\left(v^{(d)}_m \mathbf{F}_{m_i}\right) - \sum_{m=1}^{M}\left(v^{(d)}_m H^{\eta}_{m_i}\right),\ \forall i$. We also have $\sum_{m=1}^{M} v^{(d)}_m \mathbf{F}_{m_i} = \mathbf{G}^{(d)}_i$ and $\sum_{m=1}^{M} v^{(d)}_m H^{\eta}_{m_i} = \omega^{(d)}_i,\ \forall i$ due to the action of moment constraint in eq. (27) on $\mathbf{F}_{m_i}$ and $H^{\eta}_{m_i}$. Therefore, by eq. (6), $\sum_{m=1}^{M}\chi^{(d)}_{m_i} = \psi^{(d)}_i,\ \forall i$. Using this and eq. (43) in eq. (45), we obtain,

$$\left\langle [[\mathbf{V}]]_{i_d\pm\frac{1}{2}}, \mathbf{G}^{(d)^{\star}}_{i_d\pm\frac{1}{2}}\right\rangle = \left[\left[\psi^{(d)}\right]\right]_{i_d\pm\frac{1}{2}} \tag{46}$$

This proves 2.
We know that the three-point entropy equality in eq. (41) holds true corresponding to the assumptions stated in Theorem 1. Since $\sum_{m=1}^{M}(H^{\eta}_m)_i = \eta_i,\ \forall i$ (due to the action of moment constraint in eq. (26) on $(H^{\eta}_m)_i$), moment of eq. (41) gives,

$$\frac{d}{dt}\eta_i + \frac{1}{\Delta x_d}\left(\sum_{m=1}^{M}\left(v^{(d)}_m H^{\eta}_m\right)^{\star}_{i_d+\frac{1}{2}} - \sum_{m=1}^{M}\left(v^{(d)}_m H^{\eta}_m\right)^{\star}_{i_d-\frac{1}{2}}\right) = 0 \tag{47}$$

Since $\left(\partial_{\mathbf{F}_m} H^{\eta}_m\right)_i = \mathbf{V}_i = \left(\partial_{\mathbf{U}}\eta\right)_i$ is not a function of m (by eq. (31)), moment of $\left(v^{(d)}_m H^{\eta}_m\right)^{\star}_{i_d\pm\frac{1}{2}}$ given by eq. (42) yields,

$$\sum_{m=1}^{M}\left(v_m^{(d)}H_m^{\eta}\right)^{\star}_{i_d\pm\frac{1}{2}}=\frac{1}{2}\left(\mathbf{V}_i+\mathbf{V}_{i_d\pm1}\right)\cdot\sum_{m=1}^{M}\left(v_m^{(d)}\mathbf{F}_m\right)^{\star}_{i_d\pm\frac{1}{2}}-\frac{1}{2}\left(\sum_{m=1}^{M}\chi_{m_i}^{(d)}+\sum_{m=1}^{M}\chi_{m_{i_d\pm1}}^{(d)}\right)\tag{48}$$

We have already seen that $\sum_{m=1}^{M}\chi_{m_i}^{(d)}=\psi_i^{(d)},\ \forall i$. Using this and eq. (43), we obtain,

$$\sum_{m=1}^{M}\left(v_m^{(d)}H_m^{\eta}\right)^{\star}_{i_d\pm\frac{1}{2}}=\frac{1}{2}\left(\mathbf{V}_i+\mathbf{V}_{i_d\pm1}\right)\cdot\mathbf{G}^{(d)\star}_{i_d\pm\frac{1}{2}}-\frac{1}{2}\left(\psi_i^{(d)}+\psi_{i_d\pm1}^{(d)}\right)\tag{49}$$

It can be seen from eq. (10) that $\sum_{m=1}^{M}\left(v_m^{(d)}H_m^{\eta}\right)^{\star}_{i_d\pm\frac{1}{2}}=\omega^{(d)\star}_{i_d\pm\frac{1}{2}}$. This proves 3. □

In the light of eq. (31) resulting from Lemma 1, moments involved in the proof of above theorem become linear since $\partial_{\mathbf{F}_m}H_m^{\eta}$ is not a function of m. This plays a pivotal role in showing that entropy conserving scheme for vector-kinetic model results in an entropy conserving scheme for macroscopic model.

Remark 1. In the above proof, the three-point entropy equality for macroscopic model (eq. (9)) with interface numerical entropy flux $\omega^{(d)\star}_{i_d\pm\frac{1}{2}}$ given by eq. (10) is obtained as moment of three-point entropy equality for vector-kinetic model. Unlike this, we can also obtain eq. (9) directly at the macroscopic level as a consequence of $\mathbf{G}^{(d)\star}_{i_d\pm\frac{1}{2}}=\sum_{m=1}^{M}\left(v_m^{(d)}\mathbf{F}_m\right)^{\star}_{i_d\pm\frac{1}{2}}$ satisfying the entropy conserving condition for macroscopic model (eq. (8)).

The entropy conserving fluxes satisfying eq. (40) can be evaluated using an integral along the path $\mathbf{V}_{i_d+\frac{1}{2}}(\xi)=\mathbf{V}_i+\xi\Delta\mathbf{V}_{i_d+\frac{1}{2}}$ as,

$$\left(v_m^{(d)}\mathbf{F}_m\right)^{\star}_{i_d\pm\frac{1}{2}}=\int_0^1\left(v_m^{(d)}\mathbf{F}_m\right)\left(\mathbf{V}_{i_d+\frac{1}{2}}(\xi)\right)d\xi=\frac{1}{2}\left(v_m^{(d)}\mathbf{F}_{m_i}+v_m^{(d)}\mathbf{F}_{m_{i_d\pm1}}\right)-\frac{1}{2}\mathbf{Q}^{(d)\star}_{m_{i_d\pm\frac{1}{2}}}\left[[\mathbf{V}]\right]_{i_d\pm\frac{1}{2}}\tag{50}$$

where

$$\mathbf{Q}^{(d)\star}_{m_{i_d+\frac{1}{2}}}=\int_0^1(2\xi-1)\,\partial_{\mathbf{V}}\left(v_m^{(d)}\mathbf{F}_m\right)\left(\mathbf{V}_{i_d+\frac{1}{2}}(\xi)\right)d\xi\tag{51}$$

Although $\partial_{\mathbf{V}}\left(v_m^{(d)}\mathbf{F}_m\right)\left(\mathbf{V}_{i_d+\frac{1}{2}}(\xi)\right)$ is symmetric positive-definite, the term $\mathbf{Q}^{(d)\star}_{m_{i_d+\frac{1}{2}}}$ is only symmetric (need not be positive-definite). This is considered as numerical viscosity coefficient matrix that counterbalances the dispersion from average flux. Integration by parts of $\mathbf{Q}^{(d)\star}_{m_{i_d+\frac{1}{2}}}$ yields,

$$\mathbf{Q}^{(d)\star}_{m_{i_d+\frac{1}{2}}}=\int_0^1\left(\xi-\xi^2\right)\partial_{\mathbf{VV}}\left(v_m^{(d)}\mathbf{F}_m\right)\left(\mathbf{V}_{i_d+\frac{1}{2}}(\xi)\right)d\xi\left[[\mathbf{V}]\right]_{i_d\pm\frac{1}{2}}\tag{52}$$

Thus,

$$\left(v_m^{(d)}\mathbf{F}_m\right)^{\star}_{i_d\pm\frac{1}{2}}=\frac{1}{2}\left(v_m^{(d)}\mathbf{F}_{m_i}+v_m^{(d)}\mathbf{F}_{m_{i_d\pm1}}\right)+O\left(\left|\left[[\mathbf{V}]\right]_{i_d+\frac{1}{2}}\right|^2\right)\tag{53}$$

and hence for smooth functions, we have

$$\frac{1}{\Delta x_d}\left(\left(v_m^{(d)}\mathbf{F}_m\right)^{\star}_{i_d+\frac{1}{2}}-\left(v_m^{(d)}\mathbf{F}_m\right)^{\star}_{i_d-\frac{1}{2}}\right)=\frac{1}{2\Delta x_d}\left(\left(v_m^{(d)}\mathbf{F}_m\right)_{i_d+1}-\left(v_m^{(d)}\mathbf{F}_m\right)_{i_d-1}\right)+O\left(\left|\left[\left[x_d\right]\right]_{i_d+\frac{1}{2}}\right|^2\right)\tag{54}$$

Therefore, the entropy conserving scheme for vector-kinetic model given by eq. (50) is second accurate in space. However, evaluation of a closed form interface flux function using eq. (50) is algebraically tedious for a general hyperbolic system.

The closed form expression can be obtained along the same lines as macroscopic model in [41]. Let $\left\{\mathbf{l}^j_{i_d+\frac{1}{2}}\in\mathbb{R}^p\right\}_{j=1}^{p}$ and $\left\{\mathbf{r}^j_{i_d+\frac{1}{2}}\in\mathbb{R}^p\right\}_{j=1}^{p}$ be two orthogonal sets of vectors such that $\left\langle\mathbf{l}^j_{i_d+\frac{1}{2}},\mathbf{r}^k_{i_d+\frac{1}{2}}\right\rangle=\delta_{jk}$. Let $\mathbf{V}^1_{i_d+\frac{1}{2}}=\mathbf{V}_i$ and

$$\mathbf{V}^{j+1}_{i_d+\frac{1}{2}}=\mathbf{V}^j_{i_d+\frac{1}{2}}+\left\langle\mathbf{l}^j_{i_d+\frac{1}{2}},\left[[\mathbf{V}]\right]_{i_d+\frac{1}{2}}\right\rangle\mathbf{r}^j_{i_d+\frac{1}{2}}\ ;j\in\{1,2,..,p\}\tag{55}$$

Then, we have a path connecting $\mathbf{V}_i$ and $\mathbf{V}_{i_d+1}$ since

$$\mathbf{V}^{p+1}_{i_d+\frac{1}{2}} = \mathbf{V}^{1}_{i_d+\frac{1}{2}} + \sum_{j=1}^{p} \left\langle \mathbf{l}^{j}_{i_d+\frac{1}{2}}, [[\mathbf{V}]]_{i_d+\frac{1}{2}} \right\rangle \mathbf{r}^{j}_{i_d+\frac{1}{2}} = \mathbf{V}_i + [[\mathbf{V}]]_{i_d+\frac{1}{2}} = \mathbf{V}_{i_d+1} \tag{56}$$

Now, it can be seen that the numerical flux given by,

$$\left(\upsilon_m^{(d)}\mathbf{F}_m\right)^{\star}_{i_d+\frac{1}{2}} = \sum_{j=1}^{p} \frac{\chi_m^{(d)}\left(\mathbf{V}^{j+1}_{i_d+\frac{1}{2}}\right) - \chi_m^{(d)}\left(\mathbf{V}^{j}_{i_d+\frac{1}{2}}\right)}{\left\langle \mathbf{l}^{j}_{i_d+\frac{1}{2}}, [[\mathbf{V}]]_{i_d+\frac{1}{2}} \right\rangle} \mathbf{l}^{j}_{i_d+\frac{1}{2}} \tag{57}$$

satisfies the entropy conserving condition in eq. (40). However, for the purpose of numerical simulations, we use robust entropy conserving fluxes (satisfying eq. (40)) that are derived by defining averages of certain primitive variables and by balancing the coefficients corresponding to jumps in these primitive variables. These fluxes are described in section 8.

Remark 2. Higher order entropy conserving (HOEC) fluxes for vector-kinetic model can be constructed as linear combinations of second order entropy conserving fluxes derived in this paper (along the same lines as in [23] for macroscopic model). Since linear combinations are used, as a consequence of Theorem 1, the moments of HOEC fluxes for vector-kinetic model will result in HOEC fluxes for macroscopic model.

Corollary 1. *If the assumptions stated in Theorem 1 hold and entropy conserving flux of the form in eq. (50) is used, then*

$$\sum_{m=1}^{M} \mathbf{Q}^{(d)\star}_{m_{i_d\pm\frac{1}{2}}} = \mathbf{Q}^{(d)\star}_{i_d\pm\frac{1}{2}} \tag{58}$$

Proof. By eqs. (43) and (50), we obtain

$$\mathbf{G}^{(d)\star}_{i_d\pm\frac{1}{2}} = \sum_{m=1}^{M} \left(\upsilon_m^{(d)}\mathbf{F}_m\right)^{\star}_{i_d\pm\frac{1}{2}} = \frac{1}{2}\left(\mathbf{G}_i^{(d)} + \mathbf{G}_{i_d\pm1}^{(d)}\right) - \frac{1}{2}\sum_{m=1}^{M} \mathbf{Q}^{(d)\star}_{m_{i_d\pm\frac{1}{2}}} [[\mathbf{V}]]_{i_d\pm\frac{1}{2}} \tag{59}$$

since $\sum_{m=1}^{M} \upsilon_m^{(d)}\mathbf{F}_{m_i} = \mathbf{G}_i^{(d)},\ \forall i$ due to the action of moment constraint in eq. (27) on $\mathbf{F}_{m_i}$. Further,

$$\sum_{m=1}^{M} \mathbf{Q}^{(d)\star}_{m_{i_d\pm\frac{1}{2}}} = \int_0^1 (2\xi-1) \sum_{m=1}^{M} \partial_{\mathbf{V}}\left(\upsilon_m^{(d)}\mathbf{F}_m\right)\left(\mathbf{V}_{i_d+\frac{1}{2}}(\xi)\right) d\xi \tag{60}$$

and

$$\sum_{m=1}^{M} \partial_{\mathbf{V}}\left(\upsilon_m^{(d)}\mathbf{F}_m\right)\left(\mathbf{V}_{i_d+\frac{1}{2}}(\xi)\right) = \sum_{m=1}^{M} \upsilon_m^{(d)}\partial_{\mathbf{V}}\left(a_m\mathbf{U} + b_m^j\mathbf{G}^j\right)\left(\mathbf{V}_{i_d+\frac{1}{2}}(\xi)\right) = \partial_{\mathbf{V}}\mathbf{G}^{(d)}\left(\mathbf{V}_{i_d+\frac{1}{2}}(\xi)\right) \tag{61}$$

due to the action of moment constraint in eq. (27) on $\partial_{\mathbf{V}}\mathbf{F}_m$. Thus, comparing eqs. (12) and (60), we obtain $\sum_{m=1}^{M} \mathbf{Q}^{(d)\star}_{m_{i_d\pm\frac{1}{2}}} = \mathbf{Q}^{(d)\star}_{i_d\pm\frac{1}{2}}$. □

6. Entropy stable scheme for vector-kinetic model

Consider the three-point semi-discrete conservative scheme on structured grid,

$$\frac{d}{dt}\mathbf{F}_{m_i} + \frac{1}{\Delta x_d}\left(\left(\upsilon_m^{(d)}\mathbf{F}_m\right)_{i_d+\frac{1}{2}} - \left(\upsilon_m^{(d)}\mathbf{F}_m\right)_{i_d-\frac{1}{2}}\right) = \mathbf{0} \tag{62}$$

The interface numerical flux $\left(\upsilon_m^{(d)}\mathbf{F}_m\right)_{i_d\pm\frac{1}{2}}$ is given by,

$$\left(\upsilon_m^{(d)}\mathbf{F}_m\right)_{i_d\pm\frac{1}{2}} = \left(\upsilon_m^{(d)}\mathbf{F}_m\right)^{\star}_{i_d\pm\frac{1}{2}} - \frac{1}{2}\mathbf{D}^{(d)}_{m_{i_d\pm\frac{1}{2}}}\left[\left[\partial_{\mathbf{F}_m}H_m^{\eta}\right]\right]_{i_d\pm\frac{1}{2}} \tag{63}$$

Here, $\mathbf{D}^{(d)}_{m_{i_d\pm\frac{1}{2}}} = \mathbf{Q}^{(d)}_{m_{i_d\pm\frac{1}{2}}} - \mathbf{Q}^{(d)\star}_{m_{i_d\pm\frac{1}{2}}} \cdot \mathbf{Q}^{(d)}_{m_{i_d\pm\frac{1}{2}}}$ and $\mathbf{Q}^{(d)\star}_{m_{i_d\pm\frac{1}{2}}}$ are the numerical viscosity coefficient matrices corresponding to entropy stable and entropy conserving schemes respectively. $\mathbf{Q}^{(d)\star}_{m_{i_d\pm\frac{1}{2}}}$ is given by eq. (51).

Then, the inner product of eq. (62) with $\left(\partial_{\mathbf{F}_m}H_m^{\eta}\right)_i$ gives the entropy in-equality,

$$\begin{aligned}\frac{d}{dt}H^{\eta}_{m_i} + \frac{1}{\Delta x_d}&\left(\left(\upsilon_m^{(d)}H_m^{\eta}\right)_{i_d+\frac{1}{2}} - \left(\upsilon_m^{(d)}H_m^{\eta}\right)_{i_d-\frac{1}{2}}\right)\\ &= -\frac{1}{4\Delta x_d}\left(\left[\left[\partial_{\mathbf{F}_m}H_m^{\eta}\right]\right]_{i_d+\frac{1}{2}} \cdot \mathbf{D}^{(d)}_{m_{i_d+\frac{1}{2}}}\left[\left[\partial_{\mathbf{F}_m}H_m^{\eta}\right]\right]_{i_d+\frac{1}{2}} + \left[\left[\partial_{\mathbf{F}_m}H_m^{\eta}\right]\right]_{i_d-\frac{1}{2}} \cdot \mathbf{D}^{(d)}_{m_{i_d-\frac{1}{2}}}\left[\left[\partial_{\mathbf{F}_m}H_m^{\eta}\right]\right]_{i_d-\frac{1}{2}}\right) \le 0\end{aligned} \tag{64}$$

iff $\mathbf{D}^{(d)}_{m_{i_d\pm\frac{1}{2}}}$ is positive-definite. The interface numerical entropy flux $\left(v_m^{(d)}H_m^\eta\right)_{i_d+\frac{1}{2}}$ consistent with eq. (38) becomes,

$$\left(v_m^{(d)}H_m^\eta\right)_{i_d+\frac{1}{2}} = \left(v_m^{(d)}H_m^\eta\right)^\star_{i_d+\frac{1}{2}} - \frac{1}{4}\left(\left(\partial_{\mathbf{F}_m}H_m^\eta\right)_i + \left(\partial_{\mathbf{F}_m}H_m^\eta\right)_{i_d+1}\right)\cdot\mathbf{D}^{(d)}_{m_{i_d+\frac{1}{2}}}\left[\left[\partial_{\mathbf{F}_m}H_m^\eta\right]\right]_{i_d+\frac{1}{2}} \tag{65}$$

Further, let us define the interface numerical fluxes for macroscopic model as the moment of interface numerical fluxes for vector-kinetic model as,

$$\mathbf{G}^{(d)}_{i_d\pm\frac{1}{2}} = \sum_{m=1}^{M}\left(v_m^{(d)}\mathbf{F}_m\right)_{i_d\pm\frac{1}{2}} \tag{66}$$

Theorem 2. *If the three-point semi-discrete conservative scheme (eq. (62)) for vector-kinetic model with*

- $\mathbf{F}_{m_i} = a_m\mathbf{U}_i + b_m^{(d)}\mathbf{G}_i^{(d)},\ \forall i$
- *interface numerical fluxes* $\left(v_m^{(d)}\mathbf{F}_m\right)_{i_d\pm\frac{1}{2}}$ *satisfying eq. (63) and*
- *constants* a_m, $b_m^{(d)}$ *satisfying the moment constraints in eqs. (26) and (27) while rendering the positivity of eigenvalues of* $\partial_{\mathbf{U}}\mathbf{F}_m$

is used, and if the convex entropy function corresponding to it is $H^\eta_{m_i} = a_m\eta_i + b_m^{(d)}\omega_i^{(d)},\ \forall i$, *then*

1. $\sum_{m=1}^{M}$ *eq. (62) becomes*

$$\frac{d}{dt}\mathbf{U}_i + \frac{1}{\Delta x_d}\left(\mathbf{G}^{(d)}_{i_d+\frac{1}{2}} - \mathbf{G}^{(d)}_{i_d-\frac{1}{2}}\right) = \mathbf{0} \tag{67}$$

   with $\mathbf{G}^{(d)}_{i_d\pm\frac{1}{2}}$ *given by eq. (66),*
2. *the interface numerical flux* $\mathbf{G}^{(d)}_{i_d\pm\frac{1}{2}}$ *given by eq. (66) is equal to eq. (13), and*
3. *the three-point entropy in-equality for macroscopic model (eq. (14)) holds true with interface numerical entropy flux* $\omega^{(d)}_{i_d\pm\frac{1}{2}}$ *given by eq. (15).*

Proof. Due to moment constraint in eq. (26), $\sum_{m=1}^{M}\mathbf{F}_{m_i} = \mathbf{U}_i$. Therefore, $\sum_{m=1}^{M}$ eq. (62) becomes eq. (67) with $\mathbf{G}^{(d)}_{i_d\pm\frac{1}{2}}$ given by eq. (66), thus proving 1.

Since $\left(v_m^{(d)}\mathbf{F}_m\right)_{i_d\pm\frac{1}{2}}$ follows eq. (63) and $\left[\left[\partial_{\mathbf{F}_m}H_m^\eta\right]\right]_{i_d\pm\frac{1}{2}} = [[\mathbf{V}]]_{i_d\pm\frac{1}{2}} = \left[\left[\partial_{\mathbf{U}}\eta\right]\right]_{i_d\pm\frac{1}{2}}$ is not a function of m (by eq. (31)), eq. (66) becomes,

$$\mathbf{G}^{(d)}_{i_d\pm\frac{1}{2}} = \sum_{m=1}^{M}\left(v_m^{(d)}\mathbf{F}_m\right)_{i_d\pm\frac{1}{2}} = \sum_{m=1}^{M}\left(v_m^{(d)}\mathbf{F}_m\right)^\star_{i_d\pm\frac{1}{2}} - \frac{1}{2}\sum_{m=1}^{M}\mathbf{D}^{(d)}_{m_{i_d\pm\frac{1}{2}}}[[\mathbf{V}]]_{i_d\pm\frac{1}{2}} \tag{68}$$

By Theorem 1, $\sum_{m=1}^{M}\left(v_m^{(d)}\mathbf{F}_m\right)^\star_{i_d\pm\frac{1}{2}}$ satisfies entropy conserving condition in eq. (8) and hence it is equal to $\mathbf{G}^{(d)\star}_{i_d\pm\frac{1}{2}}$. We also have $\sum_{m=1}^{M}\mathbf{Q}^{(d)\star}_{m_{i_d\pm\frac{1}{2}}} = \mathbf{Q}^{(d)\star}_{i_d\pm\frac{1}{2}}$ by Corollary 1. Further, $\sum_{m=1}^{M}\mathbf{D}^{(d)}_{m_{i_d\pm\frac{1}{2}}}$ is positive-definite as $\mathbf{D}^{(d)}_{m_{i_d\pm\frac{1}{2}}}$ is positive-definite $\forall m$. Therefore, $\mathbf{D}^{(d)}_{i_d\pm\frac{1}{2}} = \sum_{m=1}^{M}\mathbf{D}^{(d)}_{m_{i_d\pm\frac{1}{2}}} = \sum_{m=1}^{M}\mathbf{Q}^{(d)}_{m_{i_d\pm\frac{1}{2}}} - \mathbf{Q}^{(d)\star}_{i_d\pm\frac{1}{2}}$ is positive-definite, and hence

$$\mathbf{G}^{(d)}_{i_d\pm\frac{1}{2}} = \mathbf{G}^{(d)\star}_{i_d\pm\frac{1}{2}} - \frac{1}{2}\mathbf{D}^{(d)}_{i_d\pm\frac{1}{2}}[[\mathbf{V}]]_{i_d\pm\frac{1}{2}} \tag{69}$$

This proves 2.

Corresponding to the assumptions stated in Theorem 2, the three-point entropy in-equality in eq. (64) holds true. Since $\sum_{m=1}^{M}(H_m^\eta)_i = \eta_i,\ \forall i$ (due to the action of moment constraint in eq. (26) on $(H_m^\eta)_i$), $\left[\left[\partial_{\mathbf{F}_m}H_m^\eta\right]\right]_{i_d\pm\frac{1}{2}} = [[\mathbf{V}]]_{i_d\pm\frac{1}{2}} = \left[\left[\partial_{\mathbf{U}}\eta\right]\right]_{i_d\pm\frac{1}{2}}$ is not a function of m (by eq. (31)) and $\sum_{m=1}^{M}\mathbf{D}^{(d)}_{m_{i_d+\frac{1}{2}}} = \mathbf{D}^{(d)}_{i_d+\frac{1}{2}}$, moment of eq. (64) gives,

$$\frac{d}{dt}\eta_i + \frac{1}{\Delta x_d}\left(\sum_{m=1}^{M}\left(v_m^{(d)}H_m^\eta\right)_{i_d+\frac{1}{2}} - \sum_{m=1}^{M}\left(v_m^{(d)}H_m^\eta\right)_{i_d-\frac{1}{2}}\right) = -\frac{1}{4\Delta x_d}\left([[\mathbf{V}]]_{i_d+\frac{1}{2}}\cdot\mathbf{D}^{(d)}_{i_d+\frac{1}{2}}[[\mathbf{V}]]_{i_d+\frac{1}{2}} + [[\mathbf{V}]]_{i_d-\frac{1}{2}}\cdot\mathbf{D}^{(d)}_{i_d-\frac{1}{2}}[[\mathbf{V}]]_{i_d-\frac{1}{2}}\right) \tag{70}$$

Since $\left[\left[\partial_{\mathbf{F}_m}H_m^\eta\right]\right]_{i_d\pm\frac{1}{2}} = [[\mathbf{V}]]_{i_d\pm\frac{1}{2}} = \left[\left[\partial_{\mathbf{U}}\eta\right]\right]_{i_d\pm\frac{1}{2}}$ and $\left(\partial_{\mathbf{F}_m}H_m^\eta\right)_i = \mathbf{V}_i = \left(\partial_{\mathbf{U}}\eta\right)_i$ are not functions of m (by eq. (31)), moment of eq. (65) yields,

$$\sum_{m=1}^{M}\left(v_m^{(d)}H_m^{\eta}\right)_{i_d+\frac{1}{2}}=\sum_{m=1}^{M}\left(v_m^{(d)}H_m^{\eta}\right)^{\star}_{i_d+\frac{1}{2}}-\frac{1}{4}\left(\mathbf{V}_i+\mathbf{V}_{i_d+1}\right)\cdot\sum_{m=1}^{M}\mathbf{D}^{(d)}_{m_{i_d+\frac{1}{2}}}\left[[\mathbf{V}]\right]_{i_d+\frac{1}{2}} \tag{71}$$

Since $\sum_{m=1}^{M}\left(v_m^{(d)}H_m^{\eta}\right)^{\star}_{i_d+\frac{1}{2}}=\omega^{(d)\star}_{i_d+\frac{1}{2}}$ (by Theorem 1) and $\sum_{m=1}^{M}\mathbf{D}^{(d)}_{m_{i_d+\frac{1}{2}}}=\mathbf{D}^{(d)}_{i_d+\frac{1}{2}}$, comparison of the above equation with eq. (15) yields $\sum_{m=1}^{M}\left(v_m^{(d)}H_m^{\eta}\right)_{i_d+\frac{1}{2}}=\omega^{(d)}_{i_d+\frac{1}{2}}$. This proves 3. □

Thus, an entropy stable scheme for vector-kinetic model results in an entropy stable scheme for macroscopic model, thanks to eq. (31) (resulting from Lemma 1) that rendered the linearity of moments in the above proof.

Remark 3. In the above proof, the three-point entropy in-equality for macroscopic model (eq. (14)) with interface numerical entropy flux $\omega^{(d)}_{i_d\pm\frac{1}{2}}$ given by eq. (15) is obtained as moment of three-point entropy in-equality for vector-kinetic model. Unlike this, we can also obtain eq. (14) directly at the macroscopic level as a consequence of $\mathbf{G}^{(d)}_{i_d\pm\frac{1}{2}}=\sum_{m=1}^{M}\left(v_m^{(d)}\mathbf{F}_m\right)_{i_d\pm\frac{1}{2}}$ satisfying the entropy stability condition for macroscopic model (eq. (13) with positive-definite $\mathbf{D}^{(d)}_{i_d\pm\frac{1}{2}}$).

6.1. High resolution scheme

Since the interface numerical flux $\left(v_m^{(d)}\mathbf{F}_m\right)_{i_d+\frac{1}{2}}$ contains a term with $[[\mathbf{V}]]_{i_d+\frac{1}{2}}$ which is $O\left(\Delta x_d\right)$, the entropy stable scheme in eq. (62) is only first order accurate in space. In order to attain higher order accuracy in space, the interface numerical flux in eq. (63) is modified as,

$$\left(v_m^{(d)}\mathbf{F}_m\right)_{i_d\pm\frac{1}{2}}=\left(v_m^{(d)}\mathbf{F}_m\right)^{\star}_{i_d\pm\frac{1}{2}}-\frac{1}{2}\mathbf{D}^{(d)}_{m_{i_d\pm\frac{1}{2}}}\left\langle\langle\mathbf{V}\rangle\right\rangle_{i_d\pm\frac{1}{2}} \tag{72}$$

where $\left\langle\langle\mathbf{V}\rangle\right\rangle_{i_d+\frac{1}{2}}=\mathbf{V}^{-}_{i_d+1}-\mathbf{V}^{+}_{i}$. Further, $\mathbf{V}^{-}_{i_d+1}=\mathbf{V}_{i_d+1}\left(x_{d_{i_d+\frac{1}{2}}}\right)$ and $\mathbf{V}^{+}_{i}=\mathbf{V}_{i}\left(x_{d_{i_d+\frac{1}{2}}}\right)$ are higher order reconstructions of $\mathbf{V}$ at interface $i_d+\frac{1}{2}$. We utilise second order reconstructions in obtaining the numerical results, and the details are provided therein section 8. The moment of eq. (72) becomes,

$$\sum_{m=1}^{M}\left(v_m^{(d)}\mathbf{F}_m\right)_{i_d\pm\frac{1}{2}}=\mathbf{G}^{(d)\star}_{i_d\pm\frac{1}{2}}-\frac{1}{2}\mathbf{D}^{(d)}_{i_d\pm\frac{1}{2}}\left\langle\langle\mathbf{V}\rangle\right\rangle_{i_d\pm\frac{1}{2}} \tag{73}$$

It can be easily seen that this is a higher order entropy stable flux for macroscopic model, and it is a consequence of linearity due to eq. (31) (resulting from Lemma 1).

7. Time discretisation

Let $\mathcal{F}_{m_i}$ be $-\frac{1}{\Delta x_d}\left(\left(v_m^{(d)}\mathbf{F}_m\right)_{i_d+\frac{1}{2}}-\left(v_m^{(d)}\mathbf{F}_m\right)_{i_d-\frac{1}{2}}\right)$ where $\left(v_m^{(d)}\mathbf{F}_m\right)_{i_d\pm\frac{1}{2}}$ is entropy conserving $\left(\left(v_m^{(d)}\mathbf{F}_m\right)^{\star}_{i_d\pm\frac{1}{2}}$ satisfying eq. (40)$\right)$ or entropy stable $\left(\left(v_m^{(d)}\mathbf{F}_m\right)_{i_d\pm\frac{1}{2}}$ satisfying eq. (63)$\right)$. Then, the semi-discrete entropy conserving/stable schemes in eqs. (39) and (62) can be represented as,

$$\frac{d}{dt}\mathbf{F}_{m_i}=\mathcal{F}_{m_i} \tag{74}$$

Since we utilise second order scheme for entropy conserving/stable spatial discretisations, a third order scheme is required for the temporal derivative so that the entropy production/dissipation due to temporal derivative will not affect the entropy conservation/stability achieved spatially. Hence, the temporal derivative in above equation is discretised using 3-stage third order strong stability preserving Runge-Kutta method (SSPRK(3,3)) [39]. After each stage of the RK method, $\mathbf{U}_i$ is evaluated using $\mathbf{U}_i=\sum_{m=1}^{M}\mathbf{F}_{m_i}$, and this is utilised in the evaluation of fluxes required for the next stage.

8. Numerical results

In this section, the entropy conserving (EC)/stable (ES) schemes are tested against various physical problems governed by scalar equations and the system of shallow water equations. For each problem, the basic ingredients such as problem description, choice of macroscopic entropy-entropy flux pair, fluxes satisfying entropy conserving/stability conditions in eqs. (40) and (63), second order reconstructions of entropy stable fluxes and CFL criteria are provided. We use the following error quantifications to study the errors in macroscopic and vector-kinetic entropies at time t.

Table 2
EOC for linear advection at $T = 2\pi$ using EC scheme with $C = 0.1$.

Number of cells, Nx	Δx_1	L_2 norm	$O(L_2)$
32	0.196349541	0.035757668	-
64	0.09817477	0.00781911	2.19
128	0.049087385	0.00140703	2.47
256	0.024543693	0.000249239	2.50

$$\text{Signed error} = \frac{\sum_i \left((.)_i^t - (.)_i^{t-\Delta t}\right)}{N} \tag{75}$$

$$\text{Absolute error} = \frac{\sum_i \left|(.)_i^t - (.)_i^{t-\Delta t}\right|}{N} \tag{76}$$

Here, N is the total number of cells or grid points in the computational domain. It can be seen that the signed error allows for cancellations of positive and negative errors present at different spatial locations. An equivalent of this with reference as $t = 0$ instead of $t - \Delta t$ is commonly used in literature in the context of global entropy preservation [34]. However, in order to understand the actual entropy preservation property of a spatially entropy preserving scheme, one needs to use the absolute error that does not allow spatial cancellations. Further, we use the signed error to identify whether the scheme is globally entropy dissipating or not. A positive signed error indicates global entropy production while negative signed error indicates global entropy dissipation. We present the numerical solutions, global entropy vs. time, and error vs. time plots for each problem.

8.1. Scalar equations

We consider scalar equations of the form,

$$\partial_t U + \partial_{x_d} G^{(d)}(U) = 0 \tag{77}$$

with initial condition $U(x_1, .., x_d, .., x_D, 0) = U_0(x_1, .., x_d, .., x_D)$. We choose suitable convex entropy-entropy flux pair specific to $G^{(d)}(U)$. The constants $a_m, b_m^{(d)}$ in eqs. (25) and (28) are chosen as described in Appendix A. The time step is chosen as

$$\Delta t \leq C \frac{\Delta x}{\lambda} \; ; \; \Delta x = min\left(\Delta x_d\right) \tag{78}$$

Here, C is the CFL number. The choice of λ is described in Appendix A. The flux

$$\left(v_m^{(d)} F_m\right)^{\star}_{i_d+\frac{1}{2}} = \frac{\chi^{(d)}_{m_{i_d+1}} - \chi^{(d)}_{m_i}}{V_{i_d+1} - V_i} \tag{79}$$

satisfies the entropy conserving condition in eq. (40). This is used when $V_{i_d+1} \neq V_i$. When $V_{i_d+1} = V_i$, we do not update the flux, as any value of flux satisfies the entropy conserving condition (eq. (40)). Here, the entropy variable is $V_i = \left(\partial_U \eta\right)_i$ and the vector-kinetic entropy flux potential is given by $\chi^{(d)}_{m_i} = V_i . \left(v_m^{(d)} F_m\right)_i - \left(v_m^{(d)} H_m^{\eta}\right)_i$.

For entropy stable scheme, we use $\mathbf{D}^{(d)}_{m_{i_d+\frac{1}{2}}} \langle\langle \mathbf{V} \rangle\rangle_{i_d+\frac{1}{2}} = \frac{1}{M} \mathbf{R}^{(d)}_{i_d+\frac{1}{2}} \mathbf{\Lambda}^{(d)}_{i_d+\frac{1}{2}} \left\langle\left\langle \widetilde{\mathbf{W}} \right\rangle\right\rangle_{i_d+\frac{1}{2}}$. For scalar equations, $\mathbf{R}^{(d)}_{i_d+\frac{1}{2}} = 1$ and $\mathbf{\Lambda}^{(d)}_{i_d+\frac{1}{2}}$ is the absolute wave speed obtained using the average (arithmetic) value of U at cells i and $i_d + 1$. We use the second order reconstruction of $\left\langle\left\langle \widetilde{\mathbf{W}} \right\rangle\right\rangle_{i_d+\frac{1}{2}}$ as explained in section 8.2.

8.1.1. Linear advection

For the one-dimensional linear advection problem with $G^{(1)}(U) = U$, we choose $\eta(U) = \frac{1}{2}U^2$, and correspondingly $\omega^{(1)}(U) = \frac{1}{2}U^2$ satisfies the compatibility condition in eq. (2). The initial condition is $U_0\left(x_1\right) = \left(sin(x_1)\right)^4$. The domain of the problem is $[0, 2\pi)$, and it is discretised using 256 uniform cells. Periodic boundary conditions are used here. Numerical solutions are obtained at $T = 2\pi$.
It can be seen from Fig. 1a that the numerical solution matches well with the exact solution. Fig. 1b shows the global entropies over time. It can be seen that the entropies remain nearly constant. The signed and absolute errors in entropies are shown in Figs. 1c and 1d respectively. Since we use second order accurate entropy conserving scheme for vector-kinetic model and Δx is of $O(10^{-2})$, we expect an absolute error of $O(10^{-4})$ in the vector-kinetic entropies. This is observed in Fig. 1d. The negative signed errors in Fig. 1c indicate that the $O(\Delta x^2)$ error is globally dissipative in nature. Due to the symmetric nature of the periodic profile, there may be cancellations in errors spatially and we observe a very low signed error of $O(10^{-12})$.
In order to study the convergence of the problem, we use very low CFL of $C = 0.1$. Second order accuracy of the scheme is evident from the results presented in Table 2. The exact solution is used as reference for the convergence study.

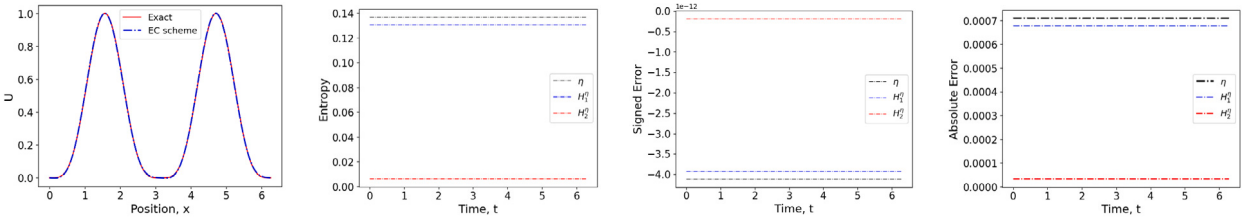

(a) Solutions (b) Entropy functions (c) Signed errors (d) Absolute errors

Fig. 1. Linear advection at $T = 2\pi$ using EC scheme with $C = 0.1$ and $Nx = 256$.

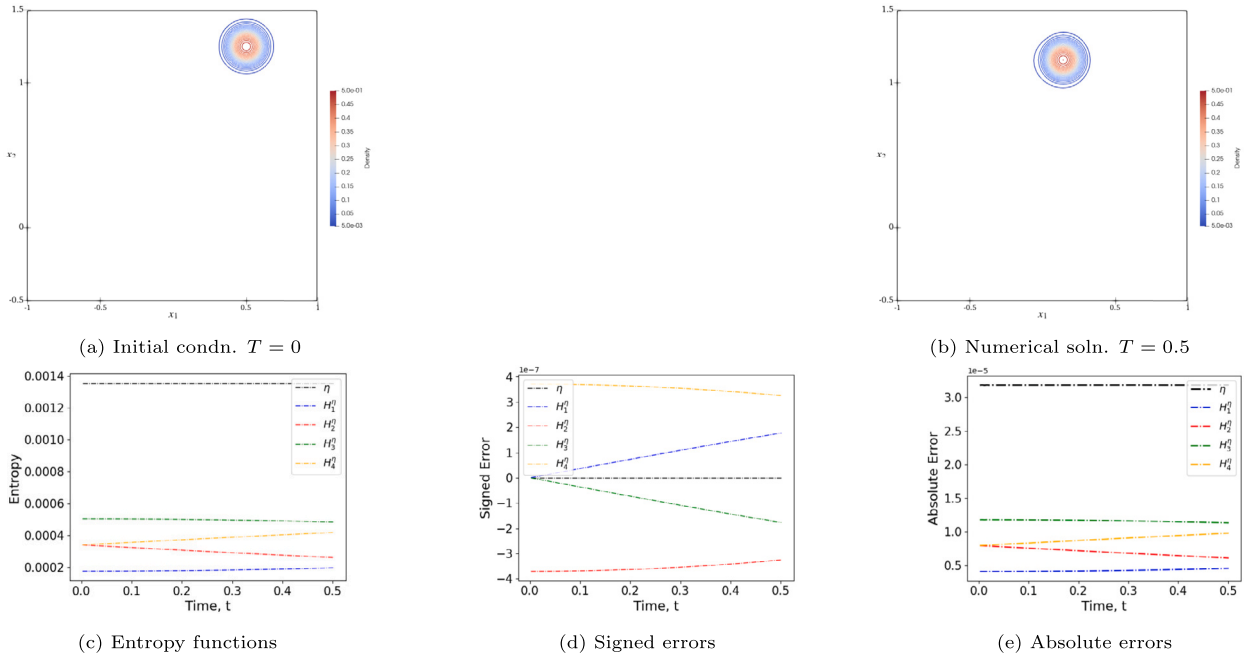

(a) Initial condn. $T = 0$ (b) Numerical soln. $T = 0.5$

(c) Entropy functions (d) Signed errors (e) Absolute errors

Fig. 2. Linear rotation at $T = 0.5$ using EC scheme with $C = 0.9$ and $Nx, Ny = 256$.

8.1.2. Linear rotation

For the two dimensional linear rotation problem, $G^{(1)}(U) = -\left(x_2 - \frac{1}{2}\right)U$ and $G^{(2)}(U) = \left(x_1 - \frac{1}{2}\right)U$. The entropy function is chosen as $\eta(U) = U^2$, and correspondingly the entropy flux functions become $\omega^{(1)}(U) = -\left(x_2 - \frac{1}{2}\right)U^2$ and $\omega^{(2)}(U) = \left(x_1 - \frac{1}{2}\right)U^2$. The initial condition is shown in Fig. 2a. The domain of the problem is $[-1, 1) \times [-0.5, 1.5)$, and it is discretised using 256×256 uniform cells. The value of U at the boundary is kept fixed throughout the computation, and a CFL of $C = 0.9$ is used.

The numerical solution at $T = 0.5$ is shown in Fig. 2b. Since Δx is of $O(10^{-2})$, one would expect an error of $O(10^{-4})$ in the absolute errors due to the usage of second order accurate entropy conserving scheme. We observe better error of $O(10^{-5})$ in Fig. 2e. Further, it is interesting to observe the symmetries in errors of H_2^η, H_4^η and H_1^η, H_3^η in Fig. 2d. However, these symmetries may not be located on the same spatial point. If they were, then the absolute error of macroscopic entropy η would be much smaller than $O(10^{-7})$ (due to cancellations) since it is the sum of vector-kinetic entropies.

8.1.3. Non-linear inviscid Burgers' test

For this non-linear one-dimensional problem with $G^{(1)}(U) = \frac{1}{2}U^2$, we choose $\eta(U) = U^2$, and correspondingly $\omega^{(1)}(U) = \frac{2}{3}U^3$ satisfies the compatibility condition in eq. (2). The initial condition is $U_0\left(x_1\right) = sin(2\pi x_1)$. The domain of the problem is $[0, 1)$, and it is discretised using 256 uniform cells. Periodic boundary conditions are used here. We use entropy conserving and entropy stable schemes respectively for obtaining numerical solutions at $T = \frac{0.1}{2\pi}$ and $T = 0.25$ in Figs. 3 and 4.

Figs. 3a and 4a show that the numerical solutions match well with the exact solutions. Figs. 3b and 4b show that macroscopic and vector-kinetic entropy functions are conserved and dissipated respectively in the smooth ($T = \frac{0.1}{2\pi}$) and non-smooth ($T = 0.25$) cases. The signed and absolute errors for $T = \frac{0.1}{2\pi}$ are shown in Figs. 3c and 3d. Since we use second order accurate entropy conserving scheme for vector-kinetic model and Δx is of $O(10^{-3})$, we expect an absolute error of $O(10^{-6})$ in the vector-kinetic entropies. However, we observe an absolute error of $O(10^{-4})$ in Fig. 1d. This might be because the terms multiplying $O(\Delta x^2)$ in the M-PDE of entropy

Table 3
EOC for non-linear inviscid Burgers' test at $T = \frac{0.1}{2\pi}$ using EC scheme with $C = 0.1$.

Number of cells, Nx	Δx_1	L_2 norm	$O(L_2)$
64	0.015625	0.000281831	-
128	0.0078125	0.000118395	1.89
256	0.00390625	4.37E-05	3.24

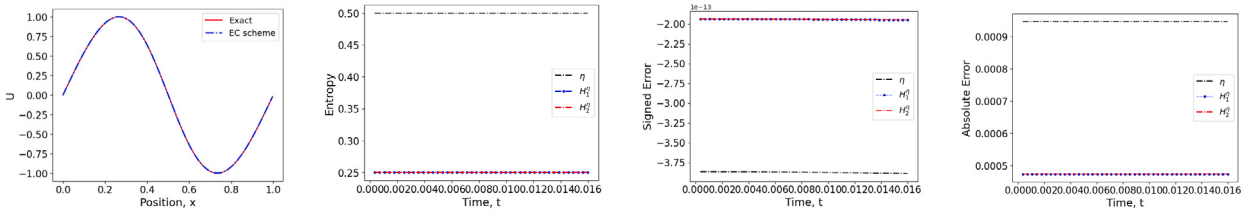

(a) Solutions (b) Entropy functions (c) Signed errors (d) Absolute errors

Fig. 3. Non-linear inviscid Burgers' test at $T = \frac{0.1}{2\pi}$ using EC scheme with $C = 0.1$ and $Nx = 256$.

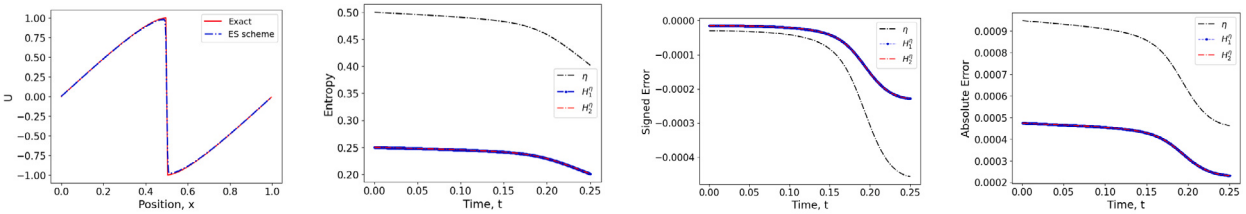

(a) Solutions (b) Entropy functions (c) Signed errors (d) Absolute errors

Fig. 4. Non-linear inviscid Burgers' test at $T = 0.25$ using first order ES scheme with $C = 0.1$ and $Nx = 256$.

equality are not $O(1)$ due to non-linearities. The negative signed errors in Fig. 1c indicate that the error is globally dissipative in nature. Due to the symmetric nature of periodic profile, there may be cancellations in errors spatially and we observe a very low signed error of $O(10^{-13})$.
Further, the signed and absolute errors for $T = 0.25$ are shown in Figs. 4c and 4d. Here too, we observe an absolute error of $O(10^{-4})$. Negative signed error of $O(10^{-4})$ indicates entropy dissipation after the formation of discontinuity.
In order to study the convergence of the problem, a very low CFL of $C = 0.1$ is chosen. The reference solution is the exact solution obtained by employing Newton-Raphson iteration with tolerance of 10^{-15}. It is seen from Table 3 that more than second order accuracy is attained as the grid is refined.

8.2. Shallow water equations

We consider the shallow water equations,

$$\partial_t \begin{bmatrix} \rho \\ \rho u_j \end{bmatrix} + \partial_{x_d} \begin{bmatrix} \rho u_d \\ \rho u_j u_d + p\delta_{dj} \end{bmatrix} = \mathbf{0} \; ; \; p = \kappa \rho^2 \; ; \; j \in \{1, 2, .., D\} \tag{80}$$

with initial condition $\mathbf{U}(x_1, .., x_d, .., x_D, 0) = \mathbf{U_0}(x_1, .., x_d, .., x_D)$. Here, $\mathbf{U} = \begin{bmatrix} \rho \\ \rho u_j \end{bmatrix}$, $\mathbf{G}^{(d)}(\mathbf{U}) = \begin{bmatrix} \rho u_d \\ \rho u_j u_d + p\delta_{dj} \end{bmatrix}$ and $\kappa = \frac{1}{2}$. The notation h, g with $h = \rho$, $g = 2\kappa = 1$ is commonly used in the shallow water community. In this case, $p = \frac{1}{2} g h^2$.
The entropy function is $\eta(\mathbf{U}) = \frac{1}{2}\rho u_j u_j + \kappa \rho^2$, and correspondingly the entropy flux functions become $\omega^{(d)}(\mathbf{U}) = u_d \left(\frac{1}{2}\rho u_j u_j + 2\kappa \rho^2 \right)$. $\mathbf{F}_m$ and H_m^η of vector-kinetic model are found using eq. (25) and eq. (28) respectively. The constants $a_m, b_m^{(d)}$ and λ are chosen as described in Appendix A. The time step is chosen as

$$\Delta t \leq C \frac{\Delta x}{\lambda} \; ; \; \Delta x = min\left(\Delta x_d\right) \tag{81}$$

Here, C is the CFL number. Let us construct the entropy conserving flux $\left(v_m^{(d)} \mathbf{F}_m \right)^\star_{i_d + \frac{1}{2}}$ satisfying eq. (40). Consider the arithmetic average $\overline{A}_{i_d + \frac{1}{2}} = \frac{1}{2}\left(A_i + A_{i_d + 1} \right)$. This average satisfies $[[AB]]_{i_d + \frac{1}{2}} = \overline{A}_{i_d + \frac{1}{2}} [[B]]_{i_d + \frac{1}{2}} + \overline{B}_{i_d + \frac{1}{2}} [[A]]_{i_d + \frac{1}{2}}$. Hence, the entropy conserving condition in eq. (40) can be expressed as,

$$\left\langle \begin{bmatrix} 2\kappa\,[[\rho]]_{i_d+\frac{1}{2}} - \overline{u_k}_{i_d+\frac{1}{2}}\left[\left[u_k\right]\right]_{i_d+\frac{1}{2}} \\ \left[\left[u_j\right]\right]_{i_d+\frac{1}{2}} \end{bmatrix}, \left(v_m^{(d)}\mathbf{F}_m\right)^{\star}_{i_d+\frac{1}{2}} \right\rangle =$$

$$v_m^{(d)}\left(2\overline{\rho}_{i_d+\frac{1}{2}}\left(a_m\,[[\rho]]_{i_d+\frac{1}{2}} + b_m^k\overline{u_k}_{i_d+\frac{1}{2}}\,[[\rho]]_{i_d+\frac{1}{2}}\right) + \overline{\rho^2}_{i_d+\frac{1}{2}}\left(b_m^k\left[\left[u_k\right]\right]_{i_d+\frac{1}{2}}\right)\right) \tag{82}$$

Equating the terms corresponding to $[[\rho]]_{i_d+\frac{1}{2}}$ and $\left[\left[u_j\right]\right]_{i_d+\frac{1}{2}}$, we obtain

$$\left(v_m^{(d)}\mathbf{F}_m\right)^{\star}_{i_d+\frac{1}{2}} = \begin{bmatrix} v_m^{(d)}\overline{\rho}_{i_d+\frac{1}{2}}\left(a_m + b_m^k\overline{u_k}_{i_d+\frac{1}{2}}\right) \\ v_m^{(d)}\left(\overline{\rho}_{i_d+\frac{1}{2}}\overline{u_j}_{i_d+\frac{1}{2}}\left(a_m + b_m^k\overline{u_k}_{i_d+\frac{1}{2}}\right) + \kappa b_m^j\overline{\rho^2}_{i_d+\frac{1}{2}}\right) \end{bmatrix} \tag{83}$$

This EC flux is second order accurate in space. Let us now derive the entropy stable flux given by eq. (63). We know that $\sum_{m=1}^{M}\mathbf{D}^{(d)}_{m_{i_d+\frac{1}{2}}} = \mathbf{D}^{(d)}_{i_d+\frac{1}{2}}$, a positive-definite matrix. We use the robust $\mathbf{D}^{(d)}_{i_d+\frac{1}{2}}$ described in [14]. That is,

$$\mathbf{D}^{(d)}_{i_d+\frac{1}{2}} = \mathbf{R}^{(d)}_{i_d+\frac{1}{2}}\mathbf{\Lambda}^{(d)}_{i_d+\frac{1}{2}}\mathbf{R}^{(d)T}_{i_d+\frac{1}{2}} \tag{84}$$

where $\mathbf{R}^{(d)}_{i_d+\frac{1}{2}}$ is a suitably scaled matrix whose columns are eigenvectors of $\partial_{\mathbf{U}}\mathbf{G}^{(d)}$, and $\mathbf{\Lambda}^{(d)}_{i_d+\frac{1}{2}}$ is the Roe-type diffusion matrix (arithmetic averages are used). The matrices $\mathbf{R}^{(d)}_{i_d+\frac{1}{2}}$ and $\mathbf{\Lambda}^{(d)}_{i_d+\frac{1}{2}}$ for shallow water equations can be found in [13]. Then, we use $\mathbf{D}^{(d)}_{m_{i_d+\frac{1}{2}}} = \frac{1}{M}\mathbf{D}^{(d)}_{i_d+\frac{1}{2}}$, $\forall m$, and these are positive-definite.

This results in a first order accurate ES flux. Let us derive the second order accurate ES flux given by eq. (72). As in [14], we express $\mathbf{D}^{(d)}_{i_d+\frac{1}{2}}\langle\langle\mathbf{V}\rangle\rangle_{i_d+\frac{1}{2}} = \mathbf{R}^{(d)}_{i_d+\frac{1}{2}}\mathbf{\Lambda}^{(d)}_{i_d+\frac{1}{2}}\left\langle\left\langle\widetilde{\mathbf{W}}\right\rangle\right\rangle_{i_d+\frac{1}{2}}$ where $\left\langle\left\langle\widetilde{\mathbf{W}}\right\rangle\right\rangle_{i_d+\frac{1}{2}} = \mathbf{B}^{(d)}_{i_d+\frac{1}{2}}\mathbf{R}^{(d)T}_{i_d+\frac{1}{2}}[[\mathbf{V}]]_{i_d+\frac{1}{2}}$. Here, $\mathbf{B}^{(d)}_{i_d+\frac{1}{2}}$ is a positive diagonal matrix. Now, consider the min-mod limiter

$$\mu(A,B) = \begin{cases} \mathrm{s}\;min(|A|,|B|) & \text{if } \mathrm{s} = sign(A) = sign(B) \\ 0 & \text{otherwise} \end{cases} \tag{85}$$

Then, the reconstruction

$$\left\langle\left\langle\widetilde{\mathbf{W}}\right\rangle\right\rangle_{i_d+\frac{1}{2}} = \mathbf{R}^{(d)T}_{i_d+\frac{1}{2}}[[\mathbf{V}]]_{i_d+\frac{1}{2}} - \frac{1}{2}\left(\mu\left(\mathbf{R}^{(d)T}_{i_d+\frac{1}{2}}[[\mathbf{V}]]_{i_d+\frac{1}{2}}, \mathbf{R}^{(d)T}_{i_d+\frac{1}{2}}[[\mathbf{V}]]_{i_{d+\frac{3}{2}}}\right) + \mu\left(\mathbf{R}^{(d)T}_{i_d+\frac{1}{2}}[[\mathbf{V}]]_{i_d-\frac{1}{2}}, \mathbf{R}^{(d)T}_{i_d+\frac{1}{2}}[[\mathbf{V}]]_{i_d+\frac{1}{2}}\right)\right) \tag{86}$$

results in a second order accurate ES flux. Since $\mathbf{B}^{(d)}_{i_d+\frac{1}{2}}$ is a positive diagonal matrix, the sign property

$$sign\left(\left\langle\left\langle\widetilde{\mathbf{W}}\right\rangle\right\rangle_{i_d+\frac{1}{2}}\right) = sign\left(\mathbf{R}^{(d)T}_{i_d+\frac{1}{2}}[[\mathbf{V}]]_{i_d+\frac{1}{2}}\right) \tag{87}$$

holds true, and the entropy stability is maintained. For vector-kinetic entropy stability, we use $\mathbf{D}^{(d)}_{m_{i_d+\frac{1}{2}}}\langle\langle\mathbf{V}\rangle\rangle_{i_d+\frac{1}{2}} = \frac{1}{M}\mathbf{D}^{(d)}_{i_d+\frac{1}{2}}\langle\langle\mathbf{V}\rangle\rangle_{i_d+\frac{1}{2}}$, $\forall m$.

It may be noted that we have derived the EC fluxes for vector-kinetic model from the vector-kinetic framework. Unlike this, we obtained the ES fluxes for vector-kinetic model based on the diffusion matrices commonly used in literature for macroscopic model. This is because the only requirement for entropy stability is positive-definiteness of $\mathbf{D}^{(d)}_{m_{i_d+\frac{1}{2}}}$, and we achieve this simply by employing the robust $\mathbf{D}^{(d)}_{i_d+\frac{1}{2}}$ used for macroscopic model.

8.2.1. 1D expansion problem

This test case is taken from [13]. The domain of the problem is $[-1,1)$, and it is discretised using 128 uniform cells. The initial condition is,

$$\rho(x_1,0) = 1,\; u_1(x_1,0) = \begin{cases} -4 & \text{if } x_1 < 0 \\ 4 & \text{if } x_1 \geq 0 \end{cases} \tag{88}$$

Since the density can become very small, non-robust schemes will crash due to the inability to maintain positivity of density. Both entropy conserving and second order entropy stable schemes do not maintain the positivity. Hence, we utilise the first order entropy stable flux for vector-kinetic model to obtain the numerical results at $T = 0.1$. The boundary values are kept fixed throughout the computation, and a very low CFL of $C = 0.1$ is used for robustness.

It can be seen from Fig. 5a that the density remains non-negative. Further, the numerical solutions of density, momentum and entropy match well with the exact solution as shown in Figs. 5a to 5c. Figs. 5d to 5f show entropy functions, their signed and absolute errors over time (for both macroscopic and vector-kinetic entropies). Since Δx is of $O(10^{-2})$, one would expect an absolute error of $O(10^{-2})$ due to the usage of first order entropy stable flux. In Fig. 5f, we observe a better absolute error of $O(10^{-3})$ in vector-kinetic entropies. Macroscopic entropy which is the sum of vector-kinetic entropies has an absolute error of $O(10^{-2})$. The negative signed errors in

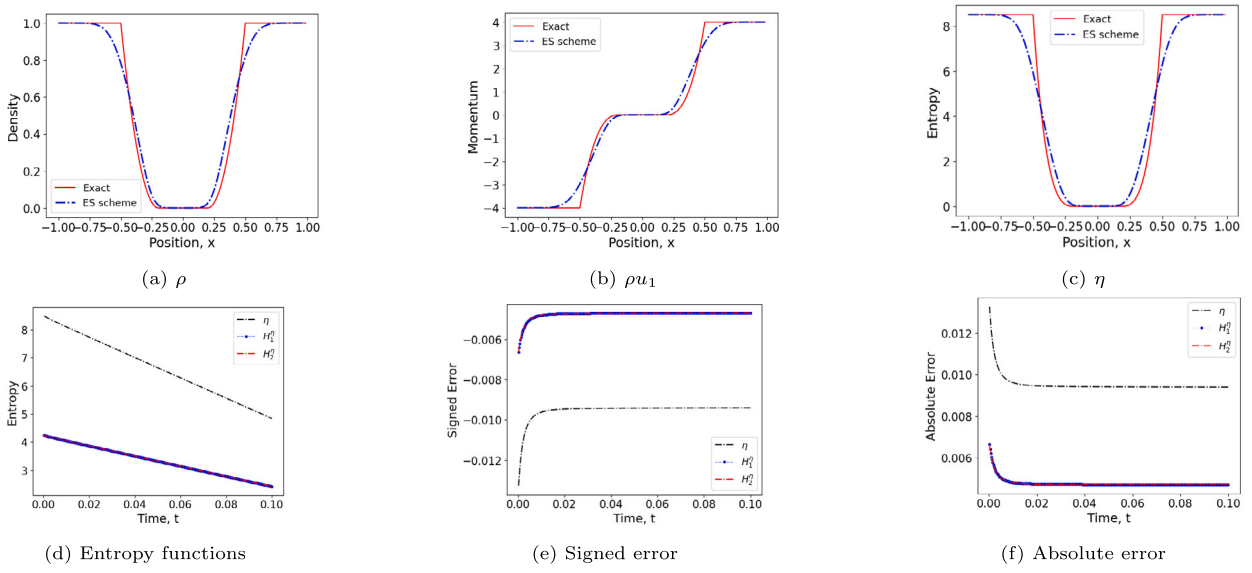

(a) ρ (b) ρu_1 (c) η

(d) Entropy functions (e) Signed error (f) Absolute error

Fig. 5. SW 1D expansion problem at $T = 0.1$ using first order ES scheme with $C = 0.1$ and $Nx = 128$.

Fig. 5e indicate the global dissipation of macroscopic and vector-kinetic entropies. This can also be seen in Fig. 5d from the decrease in global macroscopic and vector-kinetic entropies over time. It may be noted that the magnitudes of signed and absolute errors of all entropies in Figs. 5e and 5f are same. This indicates that the first order entropy stable fluxes are dissipating the entropies at almost all spatial points, and not just globally.

8.2.2. 1D dam break problem

This test case is also from [13]. The domain of the problem is $[-1, 1)$, and it is discretised using 128 uniform cells. The initial condition is,

$$\rho(x_1, 0) = \begin{cases} 15 & \text{if } x_1 < 0 \\ 1 & \text{if } x_1 \geq 0 \end{cases}, \; u_1(x_1, 0) = 0. \tag{89}$$

The numerical results obtained using first and second order entropy stable schemes at $T = 0.15$ are shown in Figs. 6 and 7 respectively. The second order entropy stable reconstruction need not produce monotone solutions near discontinuities. Hence, a minmod flux limiter (that combines first and second order entropy stable fluxes) is employed to produce monotone solution near discontinuities. The boundary values are kept fixed throughout the computation, and a CFL of $C = 0.4$ is used.

It can be seen that both first and second order (with minmod limiter) schemes capture the solution profile reasonably well. A positive signed error for H_1^η in Figs. 6e and 7e indicates that the numerical diffusion added for the flux corresponding to H_1^η is not sufficient to account for the entropy dissipation across discontinuities. This is because we have added equal weights of robust $\mathbf{D}^{(d)}_{i_d+\frac{1}{2}}$ to each of the vector-kinetic entropies, irrespective of their entropy dissipation requirements. Nevertheless, the error in macroscopic entropy which is obtained as the sum of vector-kinetic entropies is still negative (indicating entropy dissipation).

8.2.3. 2D periodic flow

This test case is taken from the literature on asymptotic preserving schemes [22]. In order to be useful in our context, we have taken the value of asymptotic parameter to be 1. The domain of the problem is $[0, 1) \times [0, 1)$, and it is discretised using 256×256 uniform cells. The initial condition shown in Fig. 8a is given by,

$$\rho(x_1, x_2, 0) = 1 + sin^2\left(2\pi\left(x_1 + x_2\right)\right) \tag{90}$$

$$u_1(x_1, x_2, 0) = u_2(x_1, x_2, 0) = sin\left(2\pi\left(x_1 - x_2\right)\right) \tag{91}$$

The numerical results obtained using entropy conserving scheme at $T = 0.1$ are shown in Fig. 8b. Periodic boundary conditions are employed, and a CFL of C = 0.5 is used. It can be seen from Fig. 8c that the macroscopic and vector-kinetic entropy functions remain almost constant over time. From Figs. 8d and 8e, we observe absolute and signed errors of $O(10^{-3})$ and $O(10^{-10})$ respectively. This huge difference implies that there are spatial cancellations between positive and negative errors. This may be due to the symmetric nature of periodic profile. Nevertheless, there is global dissipation of both macroscopic and vector-kinetic entropies as indicated by the negative errors in Fig. 8d. Order of convergence studies show that the accuracy attained is more than second order, and the results are shown in Table 4. The reference solution for convergence studies is the numerical solution with refined grid of 512×512.

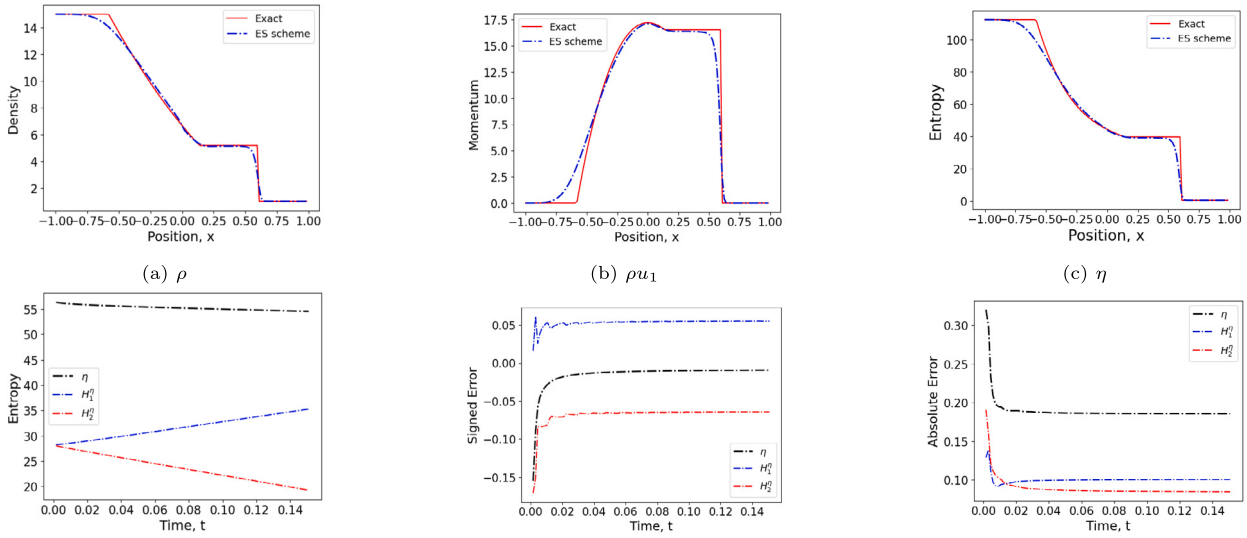

(a) ρ (b) ρu_1 (c) η

(d) Entropy functions (e) Signed errors (f) Absolute errors

Fig. 6. SW 1D dambreak problem at $T = 0.15$ using first order ES scheme with $C = 0.4$ and $Nx = 128$.

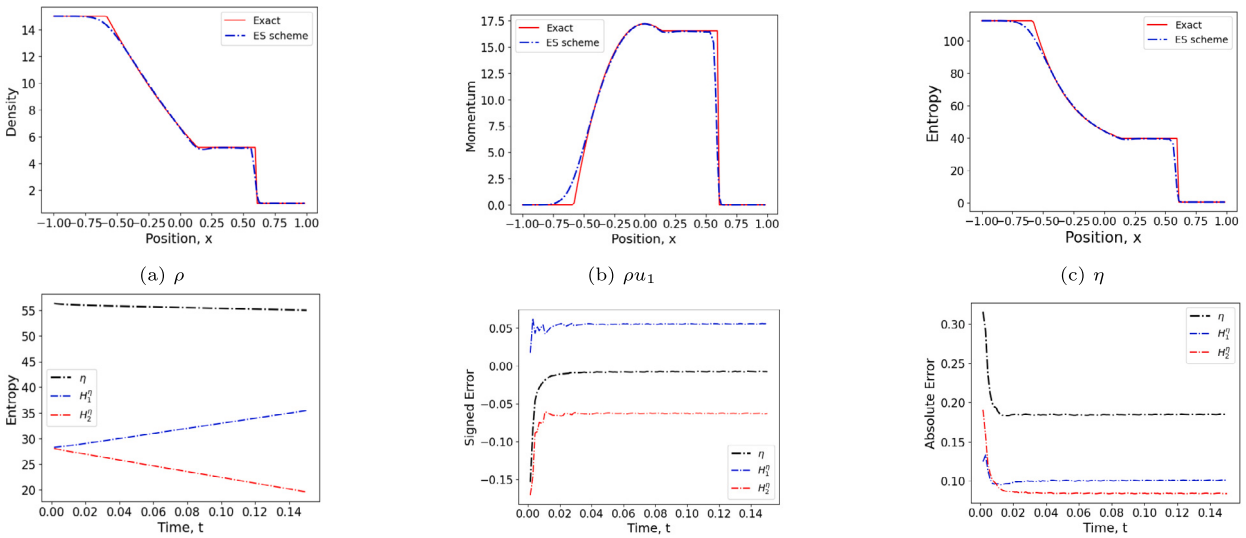

(a) ρ (b) ρu_1 (c) η

(d) Entropy functions (e) Signed errors (f) Absolute errors

Fig. 7. SW 1D dambreak problem at $T = 0.15$ using second order ES scheme (using minmod limiter) with $C = 0.4$ and $Nx = 128$.

Table 4
EOC for 2D periodic flow at $T = 0.1$ using EC scheme with $C = 0.5$.

N	Δx	$\|\|\rho\|\|_{L_2}$	$O(\|\|\rho\|\|)$	$\|\|\rho u_1\|\|_{L_2}$	$O(\|\|\rho u_1\|\|)$	$\|\|\rho u_2\|\|_{L_2}$	$O(\|\|\rho u_2\|\|)$
32	0.03125	0.00162	-	0.00255	-	0.00255	-
64	0.015625	0.000378	2.10	0.000362	2.82	0.000362	2.82
128	0.0078125	5.64×10^{-5}	2.74	5.54×10^{-5}	2.71	5.54×10^{-5}	2.71
256	0.00390625	7.62×10^{-6}	2.89	7.33×10^{-6}	2.92	7.33×10^{-6}	2.92

8.2.4. 2D travelling vortex

This test case is also taken from the literature on asymptotic preserving schemes [22]. We have taken the value of asymptotic parameter to be 0.8, so that it will be useful in our context. The domain of the problem is $[0, 1) \times [0, 1)$, and it is discretised using 256×256 uniform cells. The initial condition shown in Fig. 9a is given by,

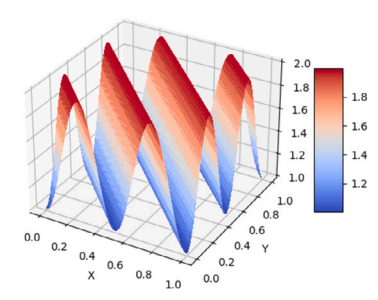

(a) Density at $T = 0$

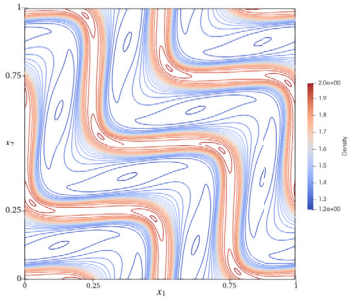

(b) Density contours at $T = 0.1$

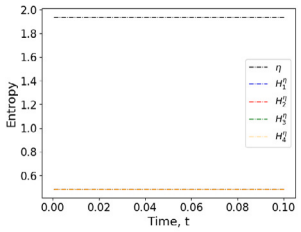

(c) Entropy functions

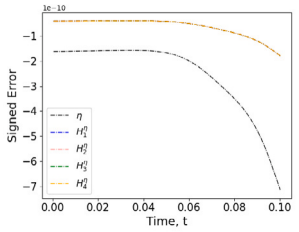

(d) Signed errors

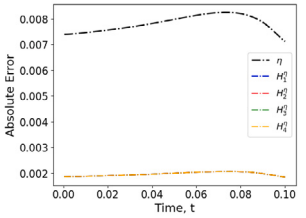

(e) Absolute errors

Fig. 8. SW 2D periodic flow at $T = 0.1$ using EC scheme with $C = 0.5$ and $Nx, Ny = 256$ (Blue, red and green lines are beneath the yellow line).

Table 5
EOC for 2D travelling vortex at $T = 0.1$ using EC scheme with $C = 0.5$.

N	Δx	$\|\|\rho\|\|_{L_2}$	$O(\|\|\rho\|\|)$	$\|\|\rho u_1\|\|_{L_2}$	$O(\|\|\rho u_1\|\|)$	$\|\|\rho u_2\|\|_{L_2}$	$O(\|\|\rho u_2\|\|)$
32	0.03125	0.000156	-	0.00339	-	0.00709	-
64	0.015625	4.39×10^{-5}	1.83	0.000505	2.75	0.00105	2.75
128	0.0078125	2.033×10^{-5}	1.11	0.000105	2.26	0.000174	2.60

$$\rho\left(x_1, x_2, 0\right) = 110 + \left(0.64\left(\frac{1.5}{4\pi}\right)^2\right) Drc\left(x_1, x_2\right)\left(k\left(rc\right) - k\left(\pi\right)\right) \tag{92}$$

$$u_1\left(x_1, x_2, 0\right) = 0.6 + 1.5\left(1 + cos\left(rc\left(x_1, x_2\right)\right)\right) Drc\left(x_1, x_2\right)\left(0.5 - x_2\right) \tag{93}$$

$$u_2\left(x_1, x_2, 0\right) = 0 + 1.5\left(1 + cos\left(rc\left(x_1, x_2\right)\right)\right) Drc\left(x_1, x_2\right)\left(x_1 - 0.5\right) \tag{94}$$

with

$$k\left(q\right) = 2cos\left(q\right) + 2q\ sin\left(q\right) + \frac{1}{8}cos\left(2q\right) + \frac{1}{4}q\ sin\left(2q\right) + \frac{3}{4}q^2 \tag{95}$$

$$rc\left(x_1, x_2\right) = 4\pi\left(\left(x_1 - 0.5\right)^2 + \left(x_2 - 0.5\right)^2\right)^{\frac{1}{2}} \tag{96}$$

$$Drc\left(x_1, x_2\right) = \begin{cases} 1 & \text{if } rc\left(x_1, x_2\right) < \pi \\ 0 & \text{otherwise} \end{cases} \tag{97}$$

The second order entropy conserving and entropy stable schemes do not distort the structure of vortex, while the first order entropy stable scheme does. We present the numerical results obtained using second order entropy conserving scheme at $T = 0.1$ as shown in Fig. 9b. Periodic boundary conditions are employed, and a CFL of C = 0.5 is used.

From Fig. 9d, we observe that the absolute errors of macroscopic and vector-kinetic entropies are of $O(10^{-3})$. On the other hand, the signed errors in H_2^η and H_4^η are of $O(10^{-11})$ (Fig. 9g), while those in H_1^η and H_3^η are of $O(10^{-5})$ (Fig. 9f). Moreover, the signed error profiles of vector-kinetic entropies are symmetric resulting in a much lower signed error of $O(10^{-14})$ for η (not shown in plot). However, these symmetries in signed errors must be located at different spatial points. If they were located at the same spatial points, then we would observe a much lower absolute error in macroscopic entropy, unlike $O(10^{-3})$ in Fig. 9d.

Order of convergence studies are shown in Table 5. It is seen that the accuracy attained is more than second order for ρu_1 and ρu_2. For ρ, the required order of accuracy is observed in coarser mesh rather than in fine mesh, and this matches the conclusion made in [37] where the analyses concerning types of vortices (based on their regularity) and their usage for validation of orders of accuracy of numerical methods are discussed.

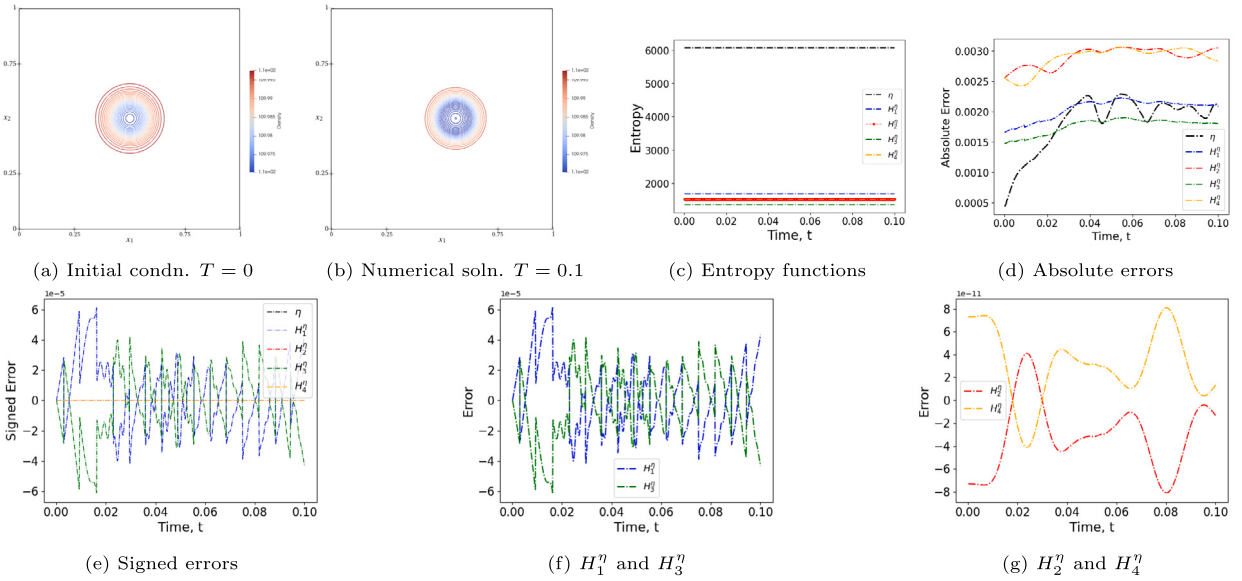

(a) Initial condn. $T = 0$ (b) Numerical soln. $T = 0.1$ (c) Entropy functions (d) Absolute errors

(e) Signed errors (f) H_1^η and H_3^η (g) H_2^η and H_4^η

Fig. 9. SW 2D travelling vortex at $T = 0.1$ using EC scheme with $C = 0.5$ and $Nx, Ny = 256$.

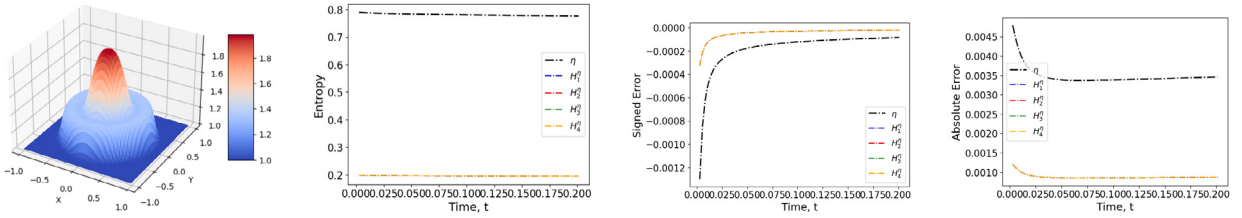

(a) Density at $T = 0.2$ (b) Entropy functions (c) Signed errors (d) Absolute errors

Fig. 10. SW 2D cylindrical dam-break at $T = 0.2$ using first order ES scheme with $C = 0.4$ and $Nx, Ny = 100$.

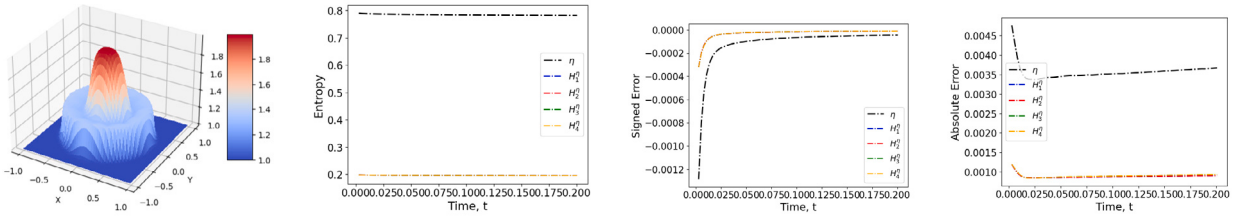

(a) Density at $T = 0.2$ (b) Entropy functions (c) Signed errors (d) Absolute errors

Fig. 11. SW 2D cylindrical dambreak at $T = 0.2$ using second order ES scheme (using minmod limiter) with $C = 0.4$ and $Nx, Ny = 100$.

8.2.5. 2D cylindrical dambreak

This test case is taken from [13]. The domain of the problem is $[-1, 1) \times [-1, 1)$, and it is discretised using 100×100 uniform cells. The initial condition is given by,

$$\rho\left(x_1, x_2, 0\right) = \begin{cases} 2 & \text{if } \left(x_1^2 + x_2^2\right)^{\frac{1}{2}} < 0.5 \\ 1 & \text{otherwise} \end{cases}, \; u_1\left(x_1, x_2, 0\right) = u_2\left(x_1, x_2, 0\right) = 0 \tag{98}$$

The numerical results of first and second order (with minmod limiter) entropy stable schemes at $T = 0.2$ are shown in Figs. 10a and 11a respectively. A CFL of $C = 0.4$ is used, and periodic boundary conditions are employed. From Figs. 10d and 11d, we observe that the absolute errors in entropies are of $O(10^{-3})$. Further, from Figs. 10c and 11c, we observe that the signed errors in entropies are of $O(10^{-4})$. The negative signed errors indicate that there is global dissipation of entropy.

9. Summary and conclusions

The following are the major highlights of the paper.

- We provided a modification to the vector-BGK model, and this allows us to obtain entropy flux potentials that are required in the consistent definition of interface numerical entropy fluxes. Lemmas 1 and 2 are essential in obtaining the entropy flux potentials.
- We showed in Theorems 1 and 2 that the moment of entropy conserving/stable schemes for vector-kinetic model results in entropy conserving/stable schemes for macroscopic model. Lemma 1 plays a crucial role by rendering the linearities in the involved moments.
- In the numerical tests of scalar smooth problems, we employed our entropy conserving scheme and observed that the macroscopic and all the vector-kinetic entropies involved are conserved (up to absolute error). We also used signed error to observe global entropy dissipation/production due to higher order terms for which conservation does not apply.
- For shallow water equations, we derived an entropy conserving flux for vector-kinetic model by considering arithmetic averages of primitive variables. We used this entropy conserving scheme on smooth problems such as periodic flow and travelling vortex. In both cases, we observed the conservation of macroscopic and vector-kinetic entropies.
- We considered the 1D expansion problem where non-positivity of density can easily occur in non-robust schemes. For this, we employed the first order entropy stable scheme for vector-kinetic model and observed that the macroscopic and all vector-kinetic entropies involved are dissipative in nature. We also do not encounter non-positivity.
- In the non-smooth category, we considered scalar non-linear inviscid Burgers' test, 1D and 2D cylindrical dam-break problems. The second order entropy stable scheme employed for scalar case dissipates macroscopic and all vector-kinetic entropies. For the shallow water case, we employed the first and second order entropy stable schemes for vector-kinetic model. In 1D dam-break problem, we observed that some of the vector-kinetic entropies are not really dissipative, as their dissipation matrices are not built based on the dissipation requirements near discontinuities. Further research is required on the choice of appropriate robust dissipation matrices for vector-kinetic model.

Thus, the entropy preserving scheme developed in this paper preserves both vector-kinetic and macroscopic entropy functions. It is interesting to observe that the entropic numerical solutions of macroscopic model do not experience a notable difference when two different routes (via vector-kinetic and macroscopic) are taken.
If the proposed entropy conserving scheme for vector-kinetic model is applied to the Euler's system, the vector-kinetic entropy conserving condition in eq. (40) can be satisfied analogous to the ways available in literature to satisfy entropy conserving condition for macroscopic model in eq. (8). One can derive the fluxes by utilising an elegant and non-costly route available in literature (for instance, by defining primitive variables, substituting for entropy variables and entropy flux potentials in terms of these primitive variables into eq. (40), and equating the coefficients of the jumps in the primitive variables, as introduced in [20] for satisfaction of the condition in eq. (8)), and this is a work in progress. It is expected that the moment of such entropy conserving flux functions for vector-kinetic model derived using a particular method (say, [20]) will be an entropy conserving flux function for macroscopic model derived using the same method ([20]).

CRediT authorship contribution statement

Megala Anandan: Conceptualization, Methodology, Formal analysis, Software, Validation, Investigation, Writing - Original draft, Reviewing and Editing.
S. V. Raghurama Rao: Conceptualization, Writing- Reviewing and Editing.

Data availability

Data will be made available on request.

Appendix A. Choice of constants $a_m, b_m^{(d)}$

We know that the moment of eq. (24) becomes the given hyperbolic system in eq. (1), if the constants $a_m, b_m^{(d)}$ in eq. (25) satisfy the moment constraints in eqs. (26) and (27). We also know that, if the convex entropy function for vector-kinetic model (eq. (28)) is used, then the moment of eq. (30) becomes eq. (3) with equality. Further, positivity of eigenvalues of $\partial_{\mathbf{U}}\mathbf{F}_m$ is an important requirement for obtaining the entropy flux potentials and the results of Theorems 1 and 2. Therefore, in order for the formulation to hold, the constants $a_m, b_m^{(d)}$ are required to satisfy eqs. (26) and (27) along with the positivity of eigenvalues of $\partial_{\mathbf{U}}\mathbf{F}_m$.
For one dimensional hyperbolic systems, we consider two discrete velocities, *i.e.,* $M = 2$. Let

$$a_1 = \frac{1}{2}, a_2 = \frac{1}{2} \tag{A.1}$$

$$b_1^{(1)} = \frac{1}{2\lambda}, b_2^{(1)} = -\frac{1}{2\lambda} \tag{A.2}$$

If $v_1^{(1)} = \lambda$ and $v_2^{(1)} = -\lambda$, then the moment constraints in eqs. (26) and (27) are satisfied. Further,

$$\text{eig}\left(\partial_{\mathbf{U}}\mathbf{F}_1\right) = \text{eig}\left(\frac{1}{2}\mathbf{I} + \frac{1}{2\lambda}\partial_{\mathbf{U}}\mathbf{G}^{(1)}\right) \tag{A.3}$$

$$\text{eig}\left(\partial_{\mathbf{U}}\mathbf{F}_2\right) = \text{eig}\left(\frac{1}{2}\mathbf{I} - \frac{1}{2\lambda}\partial_{\mathbf{U}}\mathbf{G}^{(1)}\right) \tag{A.4}$$

Thus, eigenvalues of $\partial_{\mathbf{U}}\mathbf{F}_m$ are $\frac{1}{2} \pm \frac{1}{2\lambda}\text{eig}\left(\partial_{\mathbf{U}}\mathbf{G}^{(1)}\right)$. Therefore, for positivity, we require $\lambda > \sup\left(\left|\text{eig}\left(\partial_{\mathbf{U}}\mathbf{G}^{(1)}\right)\right|\right)$. The supremum is taken over all grid points/cells in the computational domain.

For two dimensional systems, we consider four discrete velocities, *i.e.,* $M = 4$. Let

$$a_1 = \frac{1}{4}, a_2 = \frac{1}{4}, a_3 = \frac{1}{4}, a_4 = \frac{1}{4} \tag{A.5}$$

$$b_1^{(1)} = \frac{1}{2\lambda}, b_2^{(1)} = 0, b_3^{(1)} = -\frac{1}{2\lambda}, b_4^{(1)} = 0 \tag{A.6}$$

$$b_1^{(2)} = 0, b_2^{(2)} = \frac{1}{2\lambda}, b_3^{(2)} = 0, b_4^{(2)} = -\frac{1}{2\lambda} \tag{A.7}$$

If the following holds,

$$v_1^{(1)} = \lambda, v_2^{(1)} = 0, v_3^{(1)} = -\lambda, v_4^{(1)} = 0 \tag{A.8}$$

$$v_1^{(2)} = 0, v_2^{(2)} = \lambda, v_3^{(2)} = 0, v_4^{(2)} = -\lambda \tag{A.9}$$

then the moment constraints in eqs. (26) and (27) are satisfied. Further,

$$\text{eig}\left(\partial_{\mathbf{U}}\mathbf{F}_1\right) = \text{eig}\left(\frac{1}{4}\mathbf{I} + \frac{1}{2\lambda}\partial_{\mathbf{U}}\mathbf{G}^{(1)}\right) \tag{A.10}$$

$$\text{eig}\left(\partial_{\mathbf{U}}\mathbf{F}_2\right) = \text{eig}\left(\frac{1}{4}\mathbf{I} + \frac{1}{2\lambda}\partial_{\mathbf{U}}\mathbf{G}^{(2)}\right) \tag{A.11}$$

$$\text{eig}\left(\partial_{\mathbf{U}}\mathbf{F}_3\right) = \text{eig}\left(\frac{1}{4}\mathbf{I} - \frac{1}{2\lambda}\partial_{\mathbf{U}}\mathbf{G}^{(1)}\right) \tag{A.12}$$

$$\text{eig}\left(\partial_{\mathbf{U}}\mathbf{F}_4\right) = \text{eig}\left(\frac{1}{4}\mathbf{I} - \frac{1}{2\lambda}\partial_{\mathbf{U}}\mathbf{G}^{(2)}\right) \tag{A.13}$$

Thus, eigenvalues of $\partial_{\mathbf{U}}\mathbf{F}_m$ are $\frac{1}{4} \pm \frac{1}{2\lambda}\text{eig}\left(\partial_{\mathbf{U}}\mathbf{G}^{(1)}\right)$ and $\frac{1}{4} \pm \frac{1}{2\lambda}\text{eig}\left(\partial_{\mathbf{U}}\mathbf{G}^{(2)}\right)$. Therefore, for positivity, we require $\lambda > 2\sup\left(\left|\text{eig}\left(\partial_{\mathbf{U}}\mathbf{G}^{(1)}\right)\right|, \left|\text{eig}\left(\partial_{\mathbf{U}}\mathbf{G}^{(2)}\right)\right|\right)$. The supremum is taken over all grid points/cells in the domain.

References

[1] D. Aregba-Driollet, R. Natalini, Discrete kinetic schemes for multidimensional systems of conservation laws, SIAM J. Numer. Anal. 37 (6) (2000) 1973–2004.
[2] T. Barth, Numerical methods for gasdynamic systems on unstructured systems, in: M.O.D. Kröner, C. Rohde (Eds.), An Introduction to Recent Developments in Theory and Numerics for Conservation Laws, Springer, Berlin, 1999, pp. 195–285.
[3] F. Berthelin, F. Bouchut, Relaxation to isentropic gas dynamics for a BGK system with single kinetic entropy, Methods Appl. Anal. 9 (2002) 313–327.
[4] F. Bouchut, Construction of BGK models with a family of kinetic entropies for a given system of conservation laws, J. Stat. Phys. 95 (1999) 113–170.
[5] F. Bouchut, Entropy satisfying flux vector splittings and kinetic BGK models, Numer. Math. 94 (2003) 623–672.
[6] F. Bouchut, Y. Jobic, R. Natalini, R. Occelli, V. Pavan, Second-order entropy satisfying BGK-FVS schemes for incompressible Navier-Stokes equations, SMAI J. Comput. Math. 4 (2018) 1–56.
[7] J. Chan, H. Ranocha, A.M. Rueda-Ramírez, G. Gassner, T. Warburton, On the entropy projection and the robustness of high order entropy stable discontinuous Galerkin schemes for under-resolved flows, Front. Phys. 10 (2022).
[8] P. Chandrashekar, Kinetic energy preserving and entropy stable finite volume schemes for compressible Euler and Navier-Stokes equations, Commun. Comput. Phys. 14 (5) (2013) 1252–1286.
[9] P. Chandrashekar, C. Klingenberg, Entropy stable finite volume scheme for ideal compressible MHD on 2-D Cartesian meshes, SIAM J. Numer. Anal. 54 (2) (2016) 1313–1340.
[10] H. Chizari, V. Singh, F. Ismail, Cell-vertex entropy-stable finite volume methods for the system of Euler equations on unstructured grids, Comput. Math. Appl. 98 (2021) 261–279.
[11] J. Crean, J.E. Hicken, D.C. Del Rey Fernández, D.W. Zingg, M.H. Carpenter, Entropy-stable summation-by-parts discretization of the Euler equations on general curved elements, J. Comput. Phys. 356 (2018) 410–438.
[12] S.M. Deshpande, On the Maxwellian distribution, symmetric form, and entropy conservation for the Euler equations, NASA-TP-2583, L-16036, NAS 1.60:2583, 1986.
[13] U. Fjordholm, S. Mishra, E. Tadmor, Energy Preserving and Energy Stable Schemes for the Shallow Water Equations, London Mathematical Society Lecture Note Series, Cambridge University Press, 2009, pp. 93–139.
[14] U.S. Fjordholm, S. Mishra, E. Tadmor, Arbitrarily high-order accurate entropy stable essentially nonoscillatory schemes for systems of conservation laws, SIAM J. Numer. Anal. 50 (2) (2012) 544–573.
[15] G.J. Gassner, M. Svärd, F.J. Hindenlang, Stability issues of entropy-stable and/or split-form high-order schemes, J. Sci. Comput. 90 (2022) 79.
[16] G.J. Gassner, A.R. Winters, D.A. Kopriva, A well balanced and entropy conservative discontinuous Galerkin spectral element method for the shallow water equations, in: Recent Advances in Numerical Methods for Hyperbolic Partial Differential Equations, in: Applied Mathematics and Computation, vol. 272, 2016, pp. 291–308.
[17] G.J. Gassner, A.R. Winters, D.A. Kopriva, Split form nodal discontinuous Galerkin schemes with summation-by-parts property for the compressible Euler equations, J. Comput. Phys. 327 (2016) 39–66.
[18] A. Harten, On the symmetric form of systems of conservation laws with entropy, J. Comput. Phys. 49 (1) (1983) 151–164.
[19] T.J.R. Hughes, L.P. Franca, M. Mallet, A new finite element formulation for computational fluid dynamics: I. Symmetric forms of the compressible Euler and Navier—Stokes equations and the second law of thermodynamics, Appl. Mech. Eng. 54 (1986) 223–234.

[20] F. Ismail, P.L. Roe, Affordable entropy-consistent Euler flux functions II: entropy production at shocks, J. Comput. Phys. 228 (15) (2009) 5410–5436.
[21] S. Jaiswal, An entropy stable scheme for the non-linear Boltzmann equation, J. Comput. Phys. 463C (Aug 2022).
[22] K. Kaiser, J. Schütz, R. Schöbel, S. Noelle, A new stable splitting for the isentropic Euler equations, J. Sci. Comput. 70 (2017) 1390–1407.
[23] P.G. LeFloch, J.M. Mercier, C. Rohde, Fully discrete, entropy conservative schemes of arbitrary order, SIAM J. Numer. Anal. 40 (5) (2002) 1968–1992.
[24] P.G. LeFloch, H. Ranocha, Kinetic functions for nonclassical shocks, entropy stability, and discrete summation by parts, J. Sci. Comput. 87 (2020).
[25] P.L. Lions, B. Perthame, E. Tadmor, A kinetic formulation of multidimensional scalar conservation laws and related equations, J. Am. Math. Soc. 7 (1) (1994) 169–191.
[26] P.L. Lions, B. Perthame, E. Tadmor, Kinetic formulation of the isentropic gas dynamics and p-systems, Commun. Math. Phys. 163 (1994) 415–431.
[27] J. Manzanero, G. Rubio, D.A. Kopriva, E. Ferrer, E. Valero, An entropy–stable discontinuous Galerkin approximation for the incompressible Navier–Stokes equations with variable density and artificial compressibility, J. Comput. Phys. 408 (2020) 109241.
[28] R. Natalini, A discrete kinetic approximation of entropy solutions to multidimensional scalar conservation laws, J. Differ. Equ. 148 (2) (1998) 292–317.
[29] M. Parisot, Entropy-satisfying scheme for a hierarchy of dispersive reduced models of free surface flow, Int. J. Numer. Methods Fluids 91 (10) (2019) 509–531.
[30] B. Perthame, E. Tadmor, A kinetic equation with kinetic entropy functions for scalar conservation laws, Commun. Math. Phys. 136 (1991) 501–517.
[31] G. Puppo, M. Semplice, Entropy and the numerical integration of conservation laws, Phys. Proc. 00 (2011) 1–28.
[32] G. Puppo, M. Semplice, Numerical entropy and adaptivity for finite volume schemes, Commun. Comput. Phys. 10 (5) (2011) 1132–1160.
[33] H. Ranocha, L. Dalcin, M. Parsani, Fully discrete explicit locally entropy-stable schemes for the compressible Euler and Navier–Stokes equations, Comput. Math. Appl. 80 (5) (2020) 1343–1359.
[34] H. Ranocha, M. Sayyari, L. Dalcin, M. Parsani, D.I. Ketcheson, Relaxation Runge–Kutta methods: fully discrete explicit entropy-stable schemes for the compressible Euler and Navier–Stokes equations, SIAM J. Sci. Comput. 42 (2) (2020) A612–A638.
[35] D. Ray, P. Chandrashekar, Entropy stable schemes for compressible Euler equations, Int. J. Numer. Anal. Model. 4 4 (2013) 335–352.
[36] D. Ray, P. Chandrashekar, U.S. Fjordholm, S. Mishra, Entropy stable scheme on two-dimensional unstructured grids for Euler equations, Commun. Comput. Phys. 19 (5) (2016) 1111–1140.
[37] M. Ricchiuto, D. Torlo, Analytical travelling vortex solutions of hyperbolic equations for validating very high order schemes, ArXiv, arXiv:2109.10183 [abs], 2021.
[38] K.S. Shrinath, N.H. Maruthi, S.V. Raghurama Rao, V. Vasudeva Rao, A kinetic flux difference splitting method for compressible flows, Comput. Fluids 250 (2023) 105702.
[39] C.-W. Shu, S. Osher, Efficient implementation of essentially non-oscillatory shock-capturing schemes, J. Comput. Phys. 77 (2) (1988) 439–471.
[40] E. Tadmor, The numerical viscosity of entropy stable schemes for systems of conservation laws. I, Math. Comput. 49 (179) (1987) 91–103.
[41] E. Tadmor, Entropy stability theory for difference approximations of nonlinear conservation laws and related time-dependent problems, Acta Numer. 12 (2003) 451–512.
[42] E. Tadmor, Entropy stable schemes, in: R. Abgrall, C.-W. Shu (Eds.), Handbook of Numerical Methods for Hyperbolic Problems, in: Chapter 18 in Handbook of Numerical Analysis, vol. 17, Elsevier, 2016, pp. 467–493.
[43] N. Wintermeyer, A.R. Winters, G.J. Gassner, D.A. Kopriva, An entropy stable nodal discontinuous Galerkin method for the two dimensional shallow water equations on unstructured curvilinear meshes with discontinuous bathymetry, J. Comput. Phys. 340 (2017) 200–242.
[44] N.K. Yamaleev, D.C. Del Rey Fernández, J. Lou, M.H. Carpenter, Entropy stable spectral collocation schemes for the 3-D Navier-Stokes equations on dynamic unstructured grids, J. Comput. Phys. 399 (2019) 108897.
[45] G. Yan, S. Kaur, J.W. Banks, J.E. Hicken, Entropy-stable discontinuous Galerkin difference methods for hyperbolic conservation laws, J. Comput. Appl. Math. 422 (2023) 114885.